Tran-SET

Transportation Consortium of South-Central States

Solving Emerging Transportation Resiliency, Sustainability, and Economic Challenges through the Use of Innovative Materials and Construction Methods: From Research to Implementation

Evaluation of the Performance and Cost-Effectiveness of Engineered Cementitious Composites (ECC) Produced from Region 6 Local Materials

Project No. 17CLSU05

Lead University: Louisiana State University

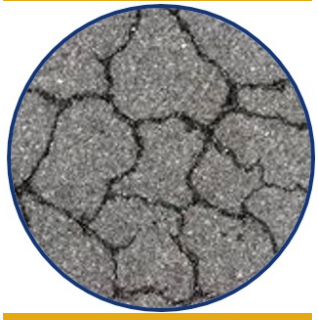

Enhancing Durability and Service Life of Infrastructure

Final Report

October 2018

Disclaimer

The contents of this report reflect the views of the authors, who are responsible for the facts and the accuracy of the information presented herein. This document is disseminated in the interest of information exchange. The report is funded, partially or entirely, by a grant from the U.S. Department of Transportation's University Transportation Centers Program. However, the U.S. Government assumes no liability for the contents or use thereof.

Acknowledgments

The authors would like to acknowledge the financial support for this study by the Transportation Consortium of South-Central States (Tran-SET) and the Louisiana Transportation Research Center (LTRC).

TECHNICAL DOCUMENTATION PAGE

1. **Project No.**	**2. Government Accession No.**	**3. Recipient's Catalog No.**
17CLSU05		

4. Title and Subtitle	**5. Report Date**
Evaluation of the Performance and Cost-Effectiveness of Engineered Cementitious Composites (ECC) Produced from Region 6 Local Materials	Oct. 2018 **6. Performing Organization Code**
7. Author(s) PI: Gabriel Arce https://orcid.org/000-0002-3610-8238 Co-PI: Tyson Rupnow https://orcid.org/0000-0002-5487-3873 Co-PI: Marwa Hassan https://orcid.org/0000-0001-8087-8232	**8. Performing Organization Report No.**
9. Performing Organization Name and Address Transportation Consortium of South-Central States (Tran-SET) University Transportation Center for Region 6 3319 Patrick F. Taylor Hall, Louisiana State University, Baton Rouge, LA 70803	**10. Work Unit No. (TRAIS)** **11. Contract or Grant No.** 69A3551747106
12. Sponsoring Agency Name and Address United States of America Department of Transportation Research and Innovative Technology Administration	**13. Type of Report and Period Covered** Final Research Report May 2017 – May 2018 **14. Sponsoring Agency Code**

15. Supplementary Notes

Report uploaded and accessible at: Tran-SET's website (http://transet.lsu.edu/)

16. Abstract

The project objective is to develop cost-effective Engineered Cementitious Composites (ECC) with locally available ingredients in Region 6 to address the deficiencies observed in ordinary concrete materials. The study explored the utilization of two types of river sands (coarse and fine), two types of PVA fibers (long and short), four levels of cement replacement with Class F fly ash, and the implementation of recycled crumb rubber in the performance of ECC materials. A total of 24 mix designs were prepared and evaluated in compression, tension, and bending to assess its mechanical properties. Furthermore, the cracking characteristics of the materials produced were evaluated to assess the durability potential of these composites. Lastly, the cost of each mix design and the feasibility of ECC implementation in transportation infrastructure were assessed. The experimental results showed that implementing crumb rubber and/or increasing contents of fly ash in the mixtures produced a positive impact in the ductility of the materials. However, a tradeoff between ductility and strength was observed. Furthermore, the utilization of the different types of sand evaluated in this study produced minor effects in the mechanical properties of ECCs evaluated. The properties of the materials developed in this study were exceedingly superior than that of regular concrete. It was concluded that ECC materials are promising for the future of transportation infrastructure.

17. Key Words	**18. Distribution Statement**
Engineered Cementitious Composites, ECC, Concrete, Pavement	No restrictions.

19. Security Classif. (of this report)	**20. Security Classif. (of this page)**	**21. No. of Pages**	**22. Price**
Unclassified	Unclassified	53	

Form DOT F 1700.7 (8-72) **Reproduction of completed page authorized.**

SI* (MODERN METRIC) CONVERSION FACTORS

APPROXIMATE CONVERSIONS TO SI UNITS

Symbol	When You Know	Multiply By	To Find	Symbol
		LENGTH		
in	inches	25.4	millimeters	mm
ft	feet	0.305	meters	m
yd	yards	0.914	meters	m
mi	miles	1.61	kilometers	km
		AREA		
in^2	square inches	645.2	square millimeters	mm^2
ft^2	square feet	0.093	square meters	m^2
yd^2	square yard	0.836	square meters	m^2
ac	acres	0.405	hectares	ha
mi^2	square miles	2.59	square kilometers	km^2
		VOLUME		
fl oz	fluid ounces	29.57	milliliters	mL
gal	gallons	3.785	liters	L
ft^3	cubic feet	0.028	cubic meters	m^3
yd^3	cubic yards	0.765	cubic meters	m^3
		NOTE: volumes greater than 1000 L shall be shown in m^3		
		MASS		
oz	ounces	28.35	grams	g
lb	pounds	0.454	kilograms	kg
T	short tons (2000 lb)	0.907	megagrams (or "metric ton")	Mg (or "t")
		TEMPERATURE (exact degrees)		
^oF	Fahrenheit	5 (F-32)/9 or (F-32)/1.8	Celsius	^oC
		ILLUMINATION		
fc	foot-candles	10.76	lux	lx
fl	foot-Lamberts	3.426	$candela/m^2$	cd/m^2
		FORCE and PRESSURE or STRESS		
lbf	poundforce	4.45	newtons	N
lbf/in^2	poundforce per square inch	6.89	kilopascals	kPa

APPROXIMATE CONVERSIONS FROM SI UNITS

Symbol	When You Know	Multiply By	To Find	Symbol
		LENGTH		
mm	millimeters	0.039	inches	in
m	meters	3.28	feet	ft
m	meters	1.09	yards	yd
km	kilometers	0.621	miles	mi
		AREA		
mm^2	square millimeters	0.0016	square inches	in^2
m^2	square meters	10.764	square feet	ft^2
m^2	square meters	1.195	square yards	yd^2
ha	hectares	2.47	acres	ac
km^2	square kilometers	0.386	square miles	mi^2
		VOLUME		
mL	milliliters	0.034	fluid ounces	fl oz
L	liters	0.264	gallons	gal
m^3	cubic meters	35.314	cubic feet	ft^3
m^3	cubic meters	1.307	cubic yards	yd^3
		MASS		
g	grams	0.035	ounces	oz
kg	kilograms	2.202	pounds	lb
Mg (or "t")	megagrams (or "metric ton")	1.103	short tons (2000 lb)	T
		TEMPERATURE (exact degrees)		
^oC	Celsius	1.8C+32	Fahrenheit	^oF
		ILLUMINATION		
lx	lux	0.0929	foot-candles	fc
cd/m^2	$candela/m^2$	0.2919	foot-Lamberts	fl
		FORCE and PRESSURE or STRESS		
N	newtons	0.225	poundforce	lbf
kPa	kilopascals	0.145	poundforce per square inch	lbf/in^2

TABLE OF CONTENTS

LIST OF FIGURES

LIST OF TABLES

ACRONYMS, ABBREVIATIONS, AND SYMBOLS

BRCC	Baton Rouge Community College
ECC	Engineered Cementitious Composites
FRC	Fiber Reinforced Concrete
HPFRCC	High Performance Fiber Reinforced Cementitious Composites
HRWR	High Range Water Reducer
LSU	Louisiana State University
LTRC	Louisiana Transportation Research Center
LVDT	Linear Variable Displacement Transducer
MOR	Modulus of Rupture
OPC	Ordinary Portland Cement
PSH	Pseudo Strain Hardening
PVA	Polyvinyl Alcohol

EXECUTIVE SUMMARY

The project focused on the development of cost-effective Engineered Cementitious Composites (ECC) with locally available ingredients in Region 6 to address the deficiencies observed in ordinary concrete materials. The study explored the utilization of two types of river sands (coarse and fine), two types of Polyvinyl Alcohol (PVA) fibers (long and short), four levels of cement replacement with Class F fly ash, and the addition of recycled crumb rubber in the performance of ECC materials. A total of 24 mix designs were produced and evaluated in compression (ASTM C39), uniaxial tension, and bending (ASTMC C1609) to assess their mechanical properties. Furthermore, a study of the cracking characteristics of the ECCs produced was conducted to evaluate the durability potential of these materials. Finally, the relative cost (compared to conventional concrete) of each mix design was examined and the feasibility of ECC implementation in transportation infrastructure was assessed.

After the experimental data was analyzed, it was found that the compressive, tensile, and flexural strengths of ECC materials were negatively affected by the implementation of crumb rubber. However, the inclusion of crumb rubber produced a remarkable increase in the tensile ductility and deflection capacity of the composites. Furthermore, crumb rubber addition produced a decrease in the average residual crack width of ECC materials providing these with an enhanced durability and self-healing potential. Similar to the effects of crumb rubber addition, increasing contents of cement replacement with fly ash also caused a decrease in the compressive, tensile and flexural strengths of ECC materials and increases in tensile ductility and deflection capacity (yet, to a lesser degree than with crumb rubber). On the other hand, utilization of the different types of sand evaluated in this study did not produce important changes in the mechanical properties of the ECC materials evaluated.

The properties of the ECC materials developed were exceedingly superior to that of regular concrete materials. For instance, one of the best performing mix design in terms of mechanical properties and cost, M-2.2 (Short-C), exhibited a compressive strength of 40.3 MPa (greater than normal strength concrete), a tensile ductility of 3.7% (370 times greater than concrete), a modulus of rupture of 11.3 MPa (more than 2 times greater than regular concrete), and a controlled average crack width of less than 65 μm (after subjecting it to its ultimate deformation capacity). Based on the exceptional properties of these materials, it was concluded that ECC materials are promising for the future of transportation infrastructure. However, research should be directed towards developing and validating (by full-scale testing) robust performance prediction models for ECC pavements. In addition, in depth, studies should be conducted to investigate the impact of jointless rigid pavements in the cost of construction as well as in repair and maintenance costs, so that highly accurate life-cycle cost assessments of ECC pavements can be conducted.

IMPLEMENTATION STATEMENT

As an outcome of this research project, several characterized ECC mix designs manufactured with locally available ingredients in Region 6 have been produced. Based on the outcomes of the project, a small-scale field study will be conducted implementing one of the best performing ECC mix designs. The field study will consist in a small repair application that will be inspected regularly until the completion of phase II. In addition, the knowledge obtained from this research project will be utilized as a foundation for a new study on ECC materials for Ultra-thin Whitetopping (UTW) application. The implementation portion of this project will also provide for internships for students from Baton Rouge Community College (BRCC) and Navajo Technical University to introduce them to research in advanced construction materials for transportation infrastructure. Furthermore, an educational module on ECC materials will be developed to be implemented in the Construction Materials course at LSU. Finally, the knowledge acquired in this investigation has been shared at national and international conferences such as the TRB Annual Meeting, Tran-SET Conference, the International Congress on Polymers in Concrete (ICPIC), and the World Transport Convention (WTC).

1. INTRODUCTION

Engineered cementitious composites (ECC) are novel fiber reinforced cementitious materials that possess high tensile ductility (as observed in Figure 1a), in the order of 100 to 500 times that of regular concrete (between 1 to 5% strain capacity in tension) *(1)*. As shown in Figure 1b, ECC have a metal-like behavior (named pseudo strain hardening) exhibiting a "yield point" (as the first cracking of the cementitious matrix occurs at about 0.01% strain) with a subsequent strain-hardening behavior. This strain hardening behavior is accompanied by multiple microcrack formation in contrast to a localized crack opening observed in concrete or typical fiber reinforced concrete (FRC) as shown in Figure 2a *(2)*. Microcracks open from zero to about 60 μm between the first cracking strain of about 0.01% and 1% where further deformation causes more microcracks formations without additional crack opening beyond the steady state value *(2-4)*. This steady state crack width is an intrinsic property of the material (which can be tailored with the use of micromechanics concepts) and is fundamental to the great durability potential of this novel material *(2)*.

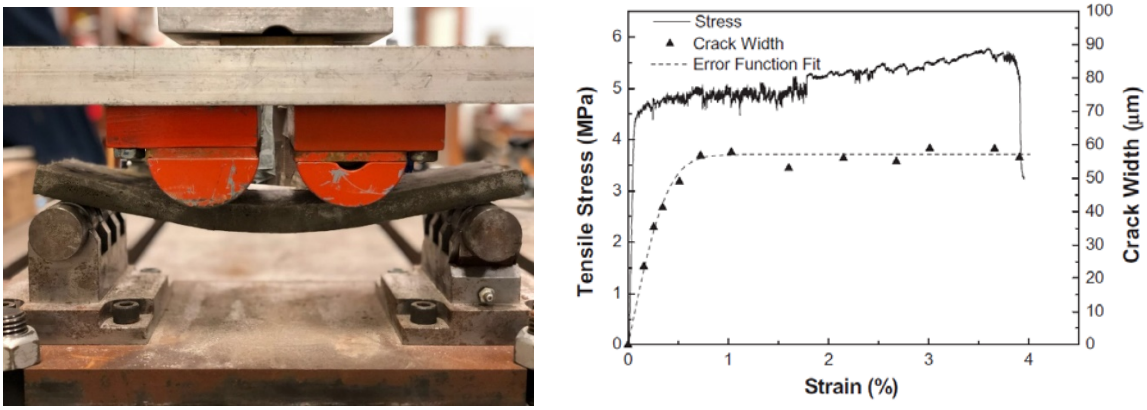

(a) (b)

Figure 1. (a) High ductility of crumb rubber ECC flexural specimen produced at LSU and (b) typical ECC uniaxial tensile test stress-strain and crack width-strain curves *(5)*.

Research on ECC durability has shown promising results in the performance against major types of concrete deterioration including corrosion, freeze-thaw, alkali silica reaction and sulfate attack *(2,6,7)*. All of which are enhanced by macroscopic cracks as well as the lack of ductility to accommodate deformation from traditional concrete materials. Furthermore, ECC also exhibits significant self-healing characteristics because of its thigh crack width that allows autogenous healing mechanisms of cementitious materials to be effective and thus enhance the durability potential of this novel material even more *(8,9)*. To date, ECC have been applied in bridge deck link slabs, bridge deck patches, and several repairs of concrete structures with successful performance *(2,10,11)*.

1.1. ECC Design

ECC are a special type of High Performance Fiber Reinforced Cementitious Composite (HPFRCC) designed and optimized by the utilization of micromechanics concepts to exhibit pseudo strain-hardening at relatively low fiber contents *(12)*. There are two basic conditions

that need to be met for the pseudo strain-hardening behavior of ECC to occur, the strength criterion and the energy criterion *(4)*. The strength criterion (Equation 1) guarantees adequate fiber bridging capacity upon crack initiation and requires the first cracking strength of the composite to be less than the fiber bridging capacity on any plausible crack plane *(4)*. On the other hand, the energy criterion (Equation 2) provides for steady-state crack propagation, which occurs when the crack tip matrix toughness (J_{tip}) is less or equal to the complementary energy of the fiber bridging relation (J'_b) *(2,4)*.

Strength criterion *(2)*:

$$\sigma_0 \geq \sigma_{cs} \quad [1]$$

where:
σ_0= Maximum fiber bridging capacity; and
σ_{cs}= Cracking strength.

Energy criterion *(2)*:

$$J'_b = \sigma_0\delta_0 - \int_0^{\delta_0} \sigma(\delta)\, d\delta \;\geq\; J_{tip} \;\approx \frac{{K_m}^2}{E_m} \quad [2]$$

where:
J'_b= Complementary energy of the fiber bridging relation;
J_{tip}= Crack tip matrix toughness;
δ_0= Crack opening corresponding to σ_0;
$\sigma(\delta)$= Fiber bridging relationship;
K_m= Matrix fracture toughness; and
E_m= Matrix Young's Modulus.

If the crack tip matrix toughness J_{tip} (sensitive to the details of the cementitious matrix design such as water/cement ratio, cement replacement with fly ash and aggregate type), is too high or inadequate energy absorption occur in the increasing phase of the σ-δ curve, then, steady-state crack propagation is hard to be achieved *(13,14)*. Figure 2b presents a graphical representation of J'_b and J_{tip} in a typical fiber bridging stress curve. The hatchet area is representative of J'_b while the shaded area is illustrative of J_{tip} (which approximates ${K_m}^2/E_m$ at low fiber contents as shown in Equation 2) *(13)*.

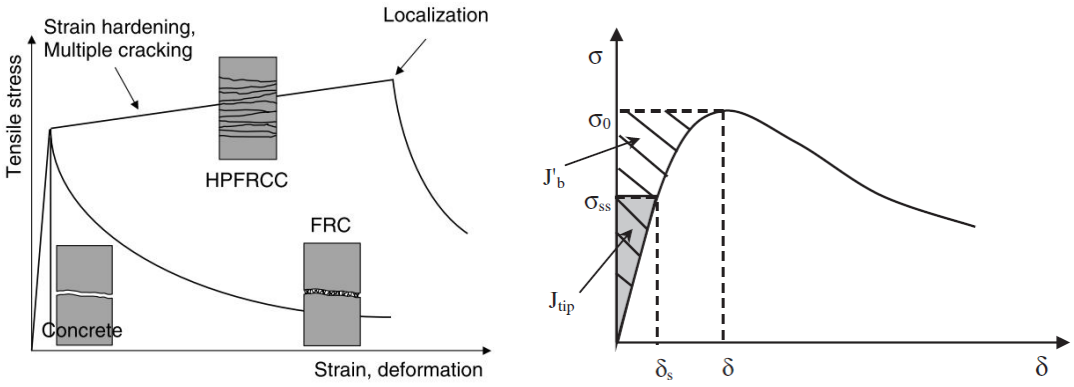

(a) (b)

Figure 2. (a) Schematic stress-strain behavior of cementitious materials in tension *(15)* and (b) typical fiber bridging stress σ vs. crack opening width δ curve *(4)*.

From Equations 1 and 2, successful design of ECC is achieved when both strength and energy criteria are satisfied. Consistent with the conditions for pseudo strain-hardening presented above, if the ratios J_b'/J_{tip} and σ_0/σ_{fc} named pseudo strain-hardening performance indexes (PSH indexes) are greater than one, both, strength and energy criteria will be met. Otherwise, if any of the two ratios is less than one, the tensile-softening behavior of fiber reinforced concrete will prevail (as shown in Figure 2a). It is important to notice that the equality signs on Equation 1 and Equation 2 assume a perfectly homogeneous material; thus, in practice the need for PSH indexes higher than one is required for robust pseudo strain-hardening performance *(2,16)*. Experimental evidence suggests that a PSH strength index of 1.45 and PSH energy index of 3 correlates to robust strain-hardening of polyvinyl alcohol (PVA) fiber reinforced cementitious composites *(16)*.

2. OBJECTIVES

The main goal of this study is to develop and characterize cost-effective ECC materials incorporating locally available ingredients by means of the following objectives:

- Develop ECC mix designs implementing locally available materials;
- Evaluate ECC mix designs mechanical properties (ultimate tensile strength and strain, flexural strength, compressive strength);
- Characterize ECC cracks (obtain crack width distribution);
- Identify key parameters affecting ECC properties; and
- Perform a feasibility study for implementation.

3. SCOPE

The proposed project is focused on the development of cost-effective Engineered Cementitious Composites (ECC) mix designs with locally available materials in Region 6 to address the deficiencies observed in ordinary concrete materials. The study explored two types of readily available river sands (coarse and fine), two types of PVA fibers (long and short), four levels of cement replacement with Class F fly ash and the addition of 20% sand replacement with recycled crumb rubber (by volume) for ECC production. Optimal ECC mix designs within the parameters explored in this study were determined based on mechanical performance, crack control, and cost. In addition, the feasibility of ECC materials for transportation infrastructure application was evaluated.

4. METHODOLOGY

4.1. Materials

Locally available ingredients were utilized in this study to produce ECC mixes: Ordinary Portland Cement (OPC) Type I, Class F Fly Ash (FA), crumb rubber with maximum particle size of 177 μm, and coarse and fine river sands with a maximum particle size of 1.18 mm (1.96 fineness modulus) and 0.6 mm (1.75 fineness modulus), respectively. The chemical compositions of cement and fly ash are presented in Table 1. It is important to notice that due to problems with materials availability, only two types of Class F Fly Ashes were utilized in this study (labelled as Fly Ash A and B). Fly Ash A was utilized in the evaluation of ECC specimens with long fibers, while Fly Ash B was used for ECC specimens with short fibers.

Table 1. Chemical composition of cement and fly ash (weight %).

Material	SiO_2	Al_2O_3	Fe_2O_3	CaO	MgO	SO_3	K_2O	TiO_2	Na_2O
Cement	19.24	4.75	3.35	65.81	2.20	3.61	0.54	0.21	-
Fly Ash A	62.08	18.56	8.22	5.69	1.69	0.37	1.42	1.03	0.35
Fly Ash B	42.68	17.44	4.06	10.90	1.94	0.81	0.94	1.25	0.25

Fibers used throughout the investigation were long RECS15 (12 mm) and short RECS15 (8 mm) polyvinyl alcohol (PVA) fibers supplied by Kuraray Co. Ltd (Japan) and NYCON (US), respectively. Table 2 presents the properties of the PVA fibers. A polycarboxylate-based high range water reducer (HRWR) was also used as an admixture.

Table 2. PVA fibers properties.

Fiber Type	Length (mm)	Diameter (μm)	Young's Modulus (GPa)	Tensile Strength (MPa)	Elongation (%)	Density (g/cm3)
Long-RECS 15	12	39	41	1600	6	1.3
Short-RECS 15	8	39	41	1600	6	1.3

4.2. Sample Preparation

Two sets of ECC specimens were prepared, regular ECC (M series) and crumb rubber ECC (MR series), where three levels of cement replacement with fly ash (by weight) were evaluated for each experimental series (62%, 69% and 75% for regular ECC series and 55%, 62%, 69% for crumb rubber ECC series). In the crumb rubber ECC experimental series, 20% of sand was replaced with crumb rubber (by volume). Furthermore, water to binder ratio (W/B) as well sand to binder ratio (S/B) were kept constant in all mix designs throughout this investigation for comparative purposes. In addition, two types of fibers (long and short) as well as two types of sands (coarse and fine) were evaluated yielding a total of 12 mix designs per experimental series. The details of the different mix proportions are summarized in Tables 3 and 4.

Table 3. Regular ECC series mix design proportions by weight.

Mix ID	Proportions by Weight									
	Cement	Fly Ash	Water	Sand	HRWR (%)[1]	W/B	S/B	FA/C	FA (%)[2]	Fibers (Vol%)
M-1.6 (Long-C)	1	1.6	0.71	0.94 (Coarse)	0.32	0.27	0.36	1.6	62	1.75 (Long)
M-2.2 (Long-C)	1	2.2	0.87	1.16 (Coarse)	0.29	0.27	0.36	2.2	69	1.75 (Long)
M-3.0 (Long-C)	1	3.0	1.09	1.45 (Coarse)	0.23	0.27	0.36	3.0	75	1.75 (Long)
M-1.6 (Long-F)	1	1.6	0.71	0.94 (Fine)	0.32	0.27	0.36	1.6	62	1.75 (Long)
M-2.2 (Long-F)	1	2.2	0.87	1.16 (Fine)	0.29	0.27	0.36	2.2	69	1.75 (Long)
M-3.0 (Long-F)	1	3.0	1.09	1.45 (Fine)	0.23	0.27	0.36	3.0	75	1.75 (Long)
M-1.6 (Short-C)	1	1.6	0.71	0.94 (Coarse)	0.32	0.27	0.36	1.6	62	1.75 (Short)
M-2.2 (Short-C)	1	2.2	0.87	1.16 (Coarse)	0.29	0.27	0.36	2.2	69	1.75 (Short)
M-3.0 (Short-C)	1	3.0	1.09	1.45 (Coarse)	0.23	0.27	0.36	3.0	75	1.75 (Short)
M-1.6 (Short-F)	1	1.6	0.71	0.94 (Fine)	0.32	0.27	0.36	1.6	62	1.75 (Short)
M-2.2 (Short-F)	1	2.2	0.87	1.16 (Fine)	0.29	0.27	0.36	2.2	69	1.75 (Short)
M-3.0 (Short-F)	1	3.0	1.09	1.45 (Fine)	0.23	0.27	0.36	3.0	75	1.75 (Short)

[1] %HRWR dosage by weight of cement
[2] % of cement replacement with fly ash by weight

The ECC mixing procedure followed in this study consisted of the following steps. Dry powder components (cement and fly ash) were mixed first in a Hobart mixer for 3 minutes. Then, sand and crumb rubber (crumb rubber experimental series) were combined with the dry powders and mixed for three additional minutes. Subsequently, water and HRWR were added and mixed for three additional minutes. Next, the rheology of the mix was assessed by means of the modified marsh funnel test proposed by Li and Li *(17)*. In this study, the consistency of each mix design was controlled to exhibit a flow number between 15 and 20 seconds. Finally, PVA fibers were introduced slowly to the wet mix (for 3 min) and mixed for an additional 7 minutes as shown in Figure 3.

Figure 3. ECC preparation and casting.

After mixing was finished, three cylindrical, prismatic and dog-bone shaped specimens were cast per each mix design (Figure 3). Subsequently, specimens were demolded after 24 hours and allowed to cure for 28 days in a moist room (23 ± 2 °C, > 95% Relative Humidity [RH]) according to ASTM C 192 *(18)*.

Table 4. Crumb rubber ECC mix design proportions by weight.

Mix ID	Proportions by Weight										
	Cement	Fly Ash	Water	Sand	HRWR (%)[1]	W/B	S/B	FA/C	FA (%)[2]	Fibers (Vol%)	CR (%)[3]
MR-1.2 (Long-C)	1	1.2	0.60	0.80 (Coarse)	0.32	0.27	0.36	1.2	55	1.75 (Long)	20
MR-1.6 (Long-C)	1	1.6	0.71	0.94 (Coarse)	0.29	0.27	0.36	1.6	62	1.75 (Long)	20
MR-2.2 (Long-C)	1	2.2	0.87	1.16 (Coarse)	0.27	0.27	0.36	2.2	69	1.75 (Long)	20
MR-1.2 (Long-F)	1	1.2	0.60	0.80 (Fine)	0.32	0.27	0.36	1.2	55	1.75 (Long)	20
MR-1.6 (Long-F)	1	1.6	0.71	0.94 (Fine)	0.29	0.27	0.36	1.6	62	1.75 (Long)	20
MR-2.2 (Long-F)	1	2.2	0.87	1.16 (Fine)	0.27	0.27	0.36	2.2	69	1.75 (Long)	20
MR-1.2 (Short-C)	1	1.2	0.60	0.80 (Coarse)	0.32	0.27	0.36	1.2	55	1.75 (Short)	20
MR-1.6 (Short-C)	1	1.6	0.71	0.94 (Coarse)	0.29	0.27	0.36	1.6	62	1.75 (Short)	20
MR-2.2 (Short-C)	1	2.2	0.87	1.16 (Coarse)	0.27	0.27	0.36	2.2	69	1.75 (Short)	20
MR-1.2 (Short-F)	1	1.2	0.60	0.80 (Fine)	0.32	0.27	0.36	1.2	55	1.75 (Short)	20
MR-1.6 (Short-F)	1	1.6	0.71	0.94 (Fine)	0.29	0.27	0.36	1.6	62	1.75 (Short)	20
MR-2.2 (Short-F)	1	2.2	0.87	1.16 (Fine)	0.27	0.27	0.36	2.2	69	1.75 (Short)	20

[1] %HRWR dosage by weight of cement

[2] % of cement replacement with fly ash by weight [3] % of sand replacement with crumb rubber by volume

4.3. ECC Testing

In order to determine the mechanical properties of the ECC materials produced, ECC specimens were tested in compression, tension and bending.

4.3.1. Compressive Strength Test

Compressive strength of ECC mix designs was evaluated according to ASTM C 39 (Compressive Strength of Cylindrical Concrete Specimens) on 101.6 x 203.2 mm (4 in x 8 in) cylindrical specimens as shown in Figure 4 *(19)*. Three specimens were prepared for each mixture to measure the compressive strength of ECC at age of 28 days. The experimental tests were performed by means of hydraulic pressure with a constant loading rate of 0.25 MPa/s.

Figure 4. Compressive strength test setup.

4.3.2. Uniaxial Tensile Test

To characterize the tensile behavior of ECC, uniaxial tensile test was conducted on dog-bone shaped specimens per recommendations of the Japan Society of Civil Engineers *(20)*. A minimum of three dog-bone specimens per mix design were cast to perform the uniaxial tensile test after 28 days of curing. A schematic of a dog-bone shaped specimen is shown in Figure 5a. The tensile tests were carried out by a 250 kN capacity MTS machine under displacement control and loading rate of 0.5 mm/min. To measure the deformation, two LVDTs were attached to each side of the specimens as illustrated in Figure 5b.

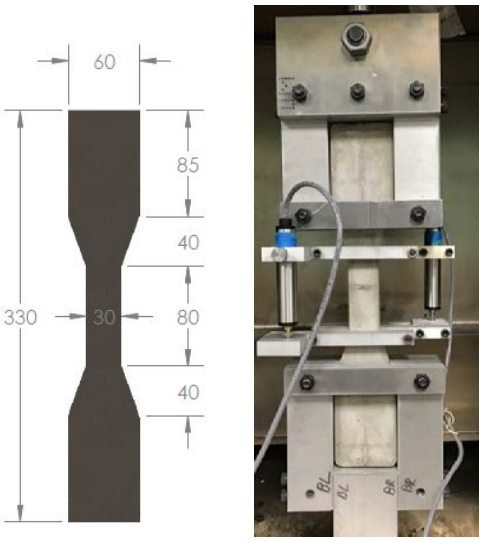

(a) (b)

Figure 5. (a) Dog-bone shaped specimen dimensions and (b) uniaxial tensile test setup.

4.3.3. Flexural Test

Third-point bending testing according to ASTM C 1609 (Flexural Performance of Fiber-Reinforced Concrete) was performed by utilizing a closed-loop, servo-controlled hydraulic universal testing system to assess flexural strength and deformation capacity of ECC mixtures *(21)*. Three prismatic specimens having dimensions of 101.6 x 101.6 x 355.6 mm (4 x 4 x 14 in) were cast for each ECC mix design. A span length of 300 mm with center span length of 100 mm was used for flexural loading. The load was applied at a rate of 0.075 mm/min. Mid-span beam net deflection and load were recorded on an automated information recording system during the third-point bending test. To measure the flexural deflection of ECC specimens, two linear variable displacement transducer (LVDT) were attached to the testing set-up. Testing setup is shown in Figure 6.

Figure 6. Third-point bending test setup.

4.4. Characterization of ECC Cracking

As previously discussed, the size of cracks in concrete materials play a key role in the durability of the material. For this reason, the cracking behavior of the ECC mix designs was studied. Right after the uniaxial tensile test was conducted; dog-bone shaped specimens were characterized using light microscopy. The width of each crack was measured at the intersection of the crack with the central axis of the specimen by digital image analysis. The microscope utilized for this study was a Zeiss SteREO Lumar V12 Microscope as shown in Figure 7.

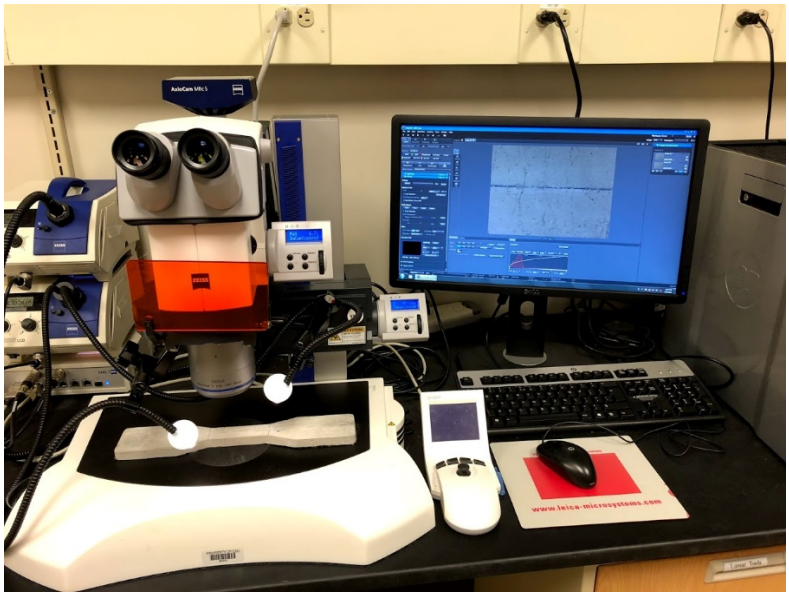

Figure 7. Zeiss SteREO Lumar V12 microscope utilized for crack analysis.

5. FINDINGS

5.1. Compressive Strength

5.1.1. Long-RECS15 Fiber

Figure 8 presents the compressive strength results of the different ECC mixtures with long RECS15 fibers. Increasing replacement of cement with fly ash (62%, 69% and 75% for regular ECC and 55%, 62% and 69% for crumb rubber ECC) decreased the compressive strength of the specimens proportionally. The strength decrease of ECC mixtures with increasing contents of fly ash could be attributed to two reasons. First, relatively high proportion of fly ash to cement may limit the secondary hydration reaction of fly ash, which may partially act as filler in the matrix (decreasing fracture toughness of the matrix). Second, the low water to binder ratio (W/B=0.27) may lead to inadequate amount of water to promote the secondary hydration reaction between cement and fly ash *(22)*.

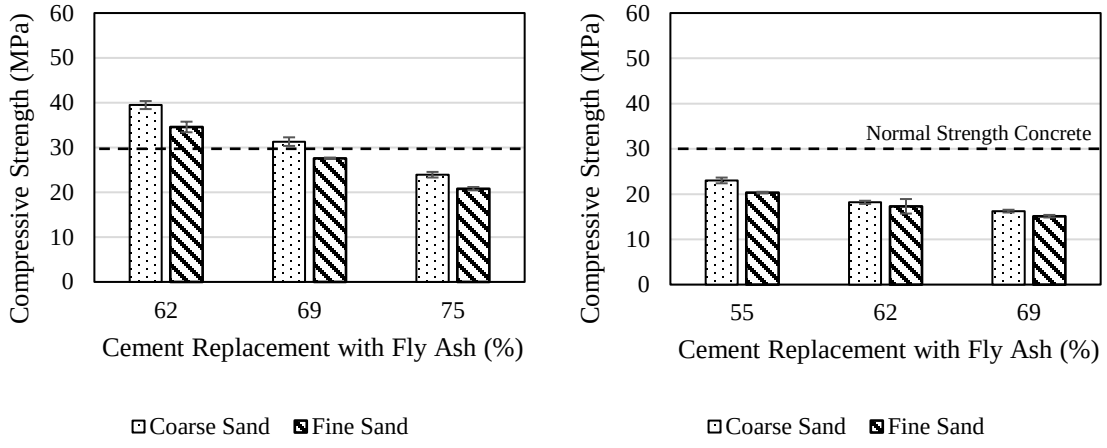

Figure 8. Compressive strength of long-RECS15 ECC: (a) regular and (b) crumb rubber.

For regular ECC specimens, the highest compressive strengths obtained with coarse and fine sand were 39.5 MPa and 34.6 MPa, respectively. These compressive strengths, which are significantly higher than the compressive strength of normal concrete (30 MPa), were achieved at 62% replacement of cement with fly ash (M-1.6). Even at a replacement of 69% of cement with fly ash (M-2.2), the compressive strength of regular ECC with coarse sand resulted in a compressive strength of 31.3 MPa, which was higher than that of regular concrete. Yet, fine sand specimens with the same fly ash content slightly underperformed the strength of regular concrete with a compressive strength of 27.6 MPa. Moreover, at the highest fly ash content of 75% replacement of cement (M-3.0), the compressive strengths obtained for coarse and fine sand specimens were of 23.9 and 20.8 MPa, respectively. It is important to notice that the strength development of fly ash in cementitious materials is usually achieved at later ages due to its pozzolanic properties; thus, significant improvements in compressive strength for high fly ash content ECC mixes like M-3.0 are expected at later ages and should be evaluated in future studies.

In the case of crumb rubber ECC experimental series, the highest compressive strengths obtained were achieved at 55% replacement of cement with fly ash (MR-1.2) with strengths of 23.0 MPa and 20.3 MPa for coarse and fine sand specimens, respectively. At 62% replacement of cement with fly ash (MR-1.6), the compressive strength of crumb rubber ECC with coarse sand was 18.2 MPa while specimens with fine sand resulted in a compressive strength of 17.3 MPa. Furthermore, at 69% replacement of cement with fly ash (MR-2.2), the compressive strengths of crumb rubber ECC with coarse sand (16.2 MPa) and fine sand (15.1 MPa) were lower than that of the minimum compressive strength for structural concrete specified by ACI 318 Standard of 17.2 MPa (2500 psi). The reduction in compressive strength of crumb rubber ECC mixes compared to the equivalent regular ECC mixes (MR-1.6 compared to M-1.6 and MR2.2 compared to M-2.2) is attributed to the defect-like behavior of crumb rubber in ECC due to its low stiffness and poor bonding with the cementitious matrix. It is recommended that future research should be directed in evaluating different dosages of crumb rubber and mixture proportions in order to mitigate excessive compressive strength reduction due to crumb rubber addition.

5.1.2. Short-RECS15 Fiber

Figure 9 presents the compressive strength results of the different ECC mixtures with short RECS15 fibers. As it was the case with Long-RECS15 specimens, increasing replacement of cement with fly ash decreased the compressive strength of the specimens proportionally. The strength decrease of ECC mixtures with increasing contents of fly ash was attributed to the same reasons discussed above in the Long-RECS15 section.

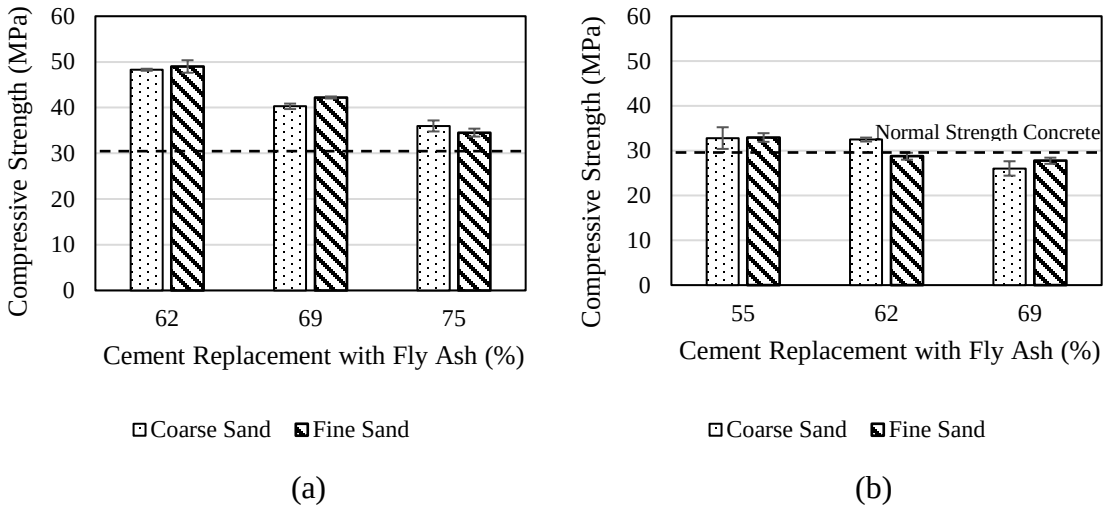

Figure 9. Compressive strength of Short-RECS15 ECC: (a) regular and (b) crumb rubber.

For regular ECC specimens, the highest compressive strengths obtained with coarse and fine sand were 48.3 MPa and 49.0 MPa, respectively. These compressive strengths, which are significantly higher than the compressive strength of normal concrete (30 MPa), were achieved at 62% replacement of cement with fly ash (M-1.6). Even at a replacement of 75% of cement with fly ash (M-3.0), the compressive strength of regular ECC with coarse and fine sand resulted in compressive strengths greater than that of regular concrete with 36.0 MPa and 34.5 MPa, respectively. It is important to notice that specimens with short RECS15 were produced

with Fly Ash B, which exhibited higher contents of CaO and lower contents of SiO_2 than that of Fly Ash A, which was utilized in the production of specimens with long RECS15 fibers. For this reason, Fly Ash B presented better cementing properties than Fly Ash A (which was more pozzolanic) yielding higher compressive strengths at 28 days.

In the case of the crumb rubber ECC experimental series, the highest compressive strengths obtained were achieved at 55% replacement of cement with fly ash (MR-1.2) with strengths of 32.8 MPa and 32.9 MPa for coarse and fine sand specimens, respectively. At 62% replacement of cement with fly ash (MR-1.6), the compressive strength of crumb rubber ECC with coarse sand was 32.5 MPa while specimens with fine sand resulted in a compressive strength 28.8 MPa (slightly lower than that of normal strength concrete). Furthermore, at 69% replacement of cement with fly ash (MR-2.2), the compressive strengths of crumb rubber ECC with coarse sand (26.0 MPa) and fine sand (27.8 MPa) were lower than that of normal strength concrete. The reduction in compressive strength of crumb rubber ECC mixes compared to the equivalent regular ECC mixes is attributed to the same causes discussed in the Long-RECS15 section above.

5.2. Uniaxial Tensile Test

5.2.1. Long-RECS15 Fiber

Figures 10 and 11 present the tensile stress vs. strain curves of each Long-RECS15 mix design evaluated in this study. As it can be observed in Figures 10 and 11, all mixes evaluated exhibited pseudo-strain hardening behavior after the first peak was reached (first cracking strength) producing significant amounts of deformation with an increase in load carrying capacity. However, material selection (crumb rubber addition and type of sand) and mix proportioning (increasing contents of fly ash) had an important impact in the tensile ductility and strength of the composites.

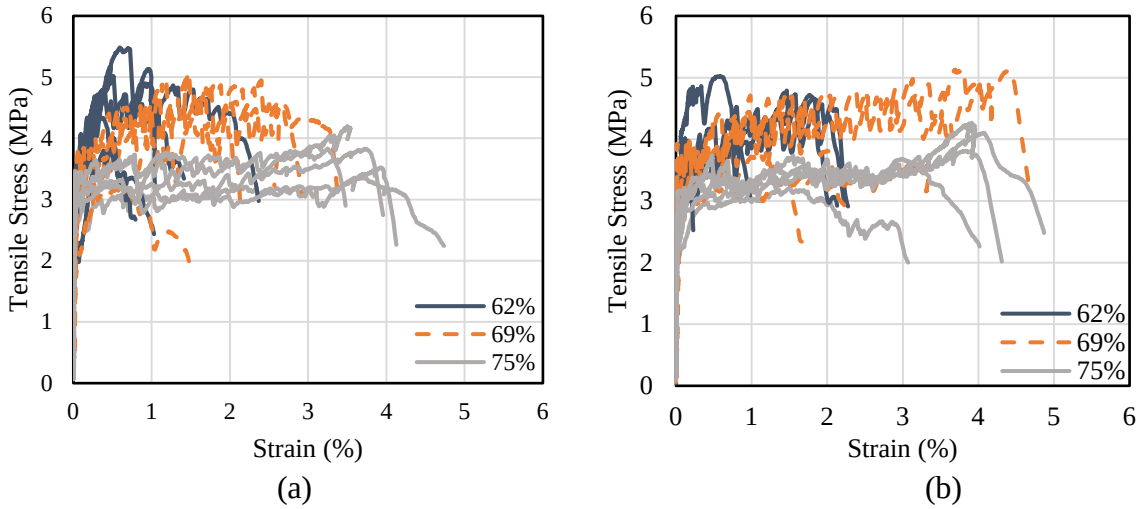

Figure 10. Tensile stress vs. strain curve of regular Long-RECS15 ECC at 62, 69 and 75% cement replacement with fly ash (a) coarse sand and (b) fine sand.

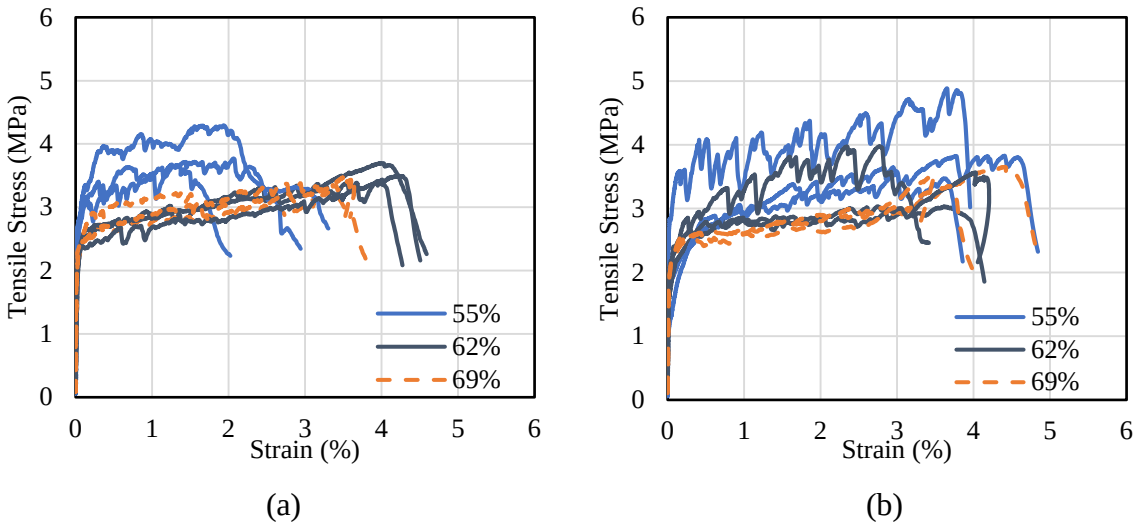

Figure 11. Tensile stress vs. strain curve of crumb rubber Long-RECS15 ECC at 55, 62 and 69% cement replacement with fly ash (a) coarse sand and (b) fine sand.

As shown in Figures 12b and 13b, the partial replacement of sand with crumb rubber (20% by volume) produced a dramatic improvement in ductility. For instance, for mix designs with 62% cement replacement with fly ash (M-1.6) the addition of crumb rubber (MR-1.6) produced an increase in tensile ductility from 0.76% to 4.06% (434% improvement) and 1.24% to 3.48% (181% improvement) for coarse and fine sand specimens, respectively. Furthermore, in the case of mixes with 69% cement replacement with fly ash (M-2.2), the addition of crumb rubber (MR-2.2) caused an increase in tensile ductility from 1.66% to 3.49% (110% improvement) and from 2.78% to 3.83% (38% improvement) for coarse and fine sand specimens, respectively.

While the ductility increases were remarkable, a decrease in the tensile strength of the composites due to the addition of crumb rubber was noticeable as shown in Figures 12a and 13a. In the case of the mixes with a 62% cement replacement with fly ash, the drop in tensile strength was from 4.80 MPa to 3.54 MPa (26% decrease) and 4.71 MPa to 3.55 MPa (25% decrease) for coarse and fine sand specimens, respectively. Moreover, for the specimens with 69% cement replacement with fly ash, the drop in tensile strength was from 4.60 MPa to 3.39 MPa (26% decrease) and 4.47 MPa to 3.53 MPa (21% decrease) for coarse and fine sand specimens, respectively. The remarkable increase in ductility provided by the addition of crumb rubber is associated to the pseudo strain hardening performance indicators PSH strength (σ_0/σ_{cs}) and PSH energy (J'_b/J_{tip}). When adding crumb rubber, the complementary energy of the fiber bridging relation J'_b tends to increase while the crack tip toughness of the cementitious matrix J_{tip} is reduced *(4)*. This produces an increment in the PSH energy index (J'_b/J_{tip}) leading to a substantial increase in ductility. In addition, the implementation of crumb rubber also produces a decrease in the fiber bridging capacity σ_0 leading to the tensile strength decrease observed *(4)*.

In contrast to the effect of crumb rubber in ECC performance, the effect of the different type of sands used in this study were minor. In terms of strength, differences in performance

between the coarse and fine sand were found to be negligible. Yet, in terms of ductility, the utilization of the finer sand tended to favor ductility, particularly when low fly ash contents where utilized. Typically, the propagation path of cracks increases in tortuosity as the aggregate size increase; thus, resulting in a higher matrix fracture toughness *(3)*. For this reason, utilization of finer sand is beneficial for increasing the ductility of ECC since it decreases the crack tip toughness of the cementitious matrix (J_{tip}); thus, enhancing the energy PSH energy index (J'_b / J_{tip}).

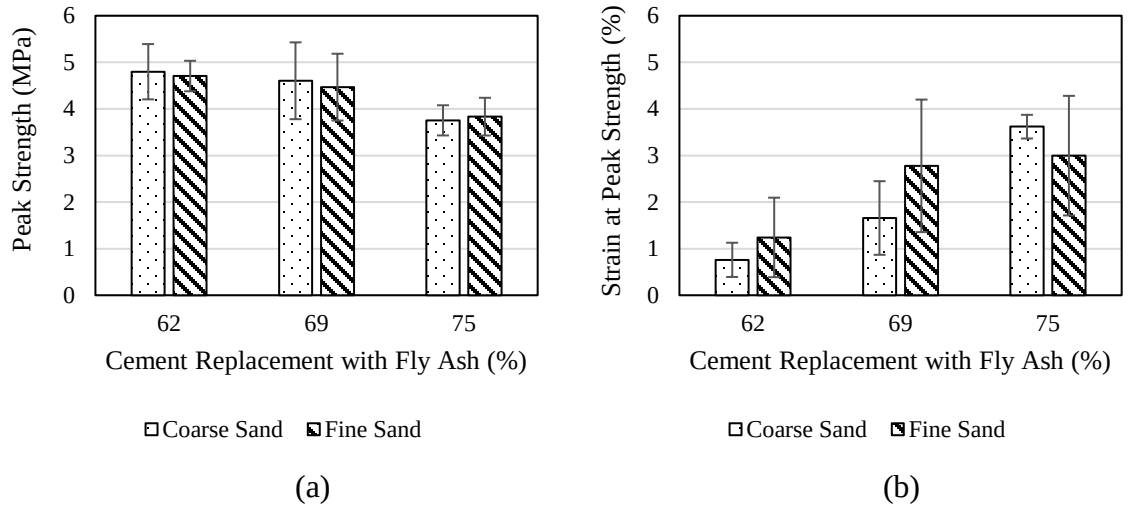

Figure 12. Uniaxial tensile test results of regular Long-RECS15 ECC: (a) peak strength and (b) strain at peak strength.

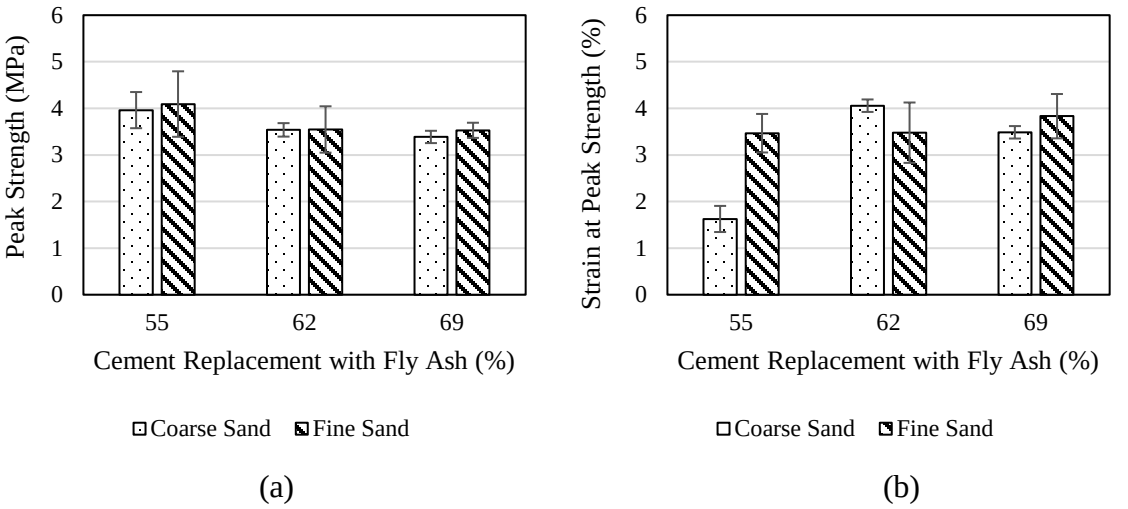

Figure 13. Uniaxial tensile test results of crumb rubber Long-RECS15 ECC: (a) peak strength and (b) strain at peak strength.

As shown in Figures 12 and 13, changes in the mix proportions considered in this study (different levels of cement replacement with fly ash) were also a relevant factor affecting the tensile properties of the ECC materials. The trend observed was that higher cement replacements with fly ash led to an increase in tensile ductility (except for MR-2.2 (69%) compared to MR-1.6 (62%) for coarse sand); however, it reduced tensile strengths. The

improvement in ductility with increasing contents of fly ash were attributed to a similar phenomenon than that occurring with crumb rubber addition. The increase in cement replacement with fly ash produces an increase in the complementary energy of the fiber bridging relation J'_b and a reduction in the crack tip toughness of the cementitious matrix J_{tip} *(4)*. In turn, this leads to an increasing PSH energy index (J'_b / J_{tip}) with increasing contents of fly ash providing the improvement in tensile ductility. However, increasing contents of fly ash also produces a decrease in the fiber bridging capacity (σ_0) of the composite leading to a decrease in tensile strength *(4)*.

Statistical analysis conducted according to ANOVA and Tukey-Kramer HSD showed statistically significant differences in the tensile ductility of regular ECC when fly ash contents were increased from 62% to 75% and from 69% to 75% for specimens utilizing coarse sand. However, this was not the case for fine sand specimens where statistical significance was not found likely due smaller differences and high variability. High variability in tensile ductility was attributed to relatively low PSH indexes possibly associated with some ECC materials evaluated. Furthermore, for crumb rubber ECC materials, significant differences in tensile ductility were found when fly ash contents were increased from 55% to 62% and from 55% to 69% for coarse sand specimens. Yet, similar to the case of regular ECC specimens, no statistical significance was found for fine sand specimens (likely due to a more uniform performance in tensile ductility observed for fine sand specimens with crumb rubber). In addition, a statistically significant difference in tensile ductility between coarse and fine sand crumb rubber ECC specimens containing 55% cement replacement with fly ash was also found. This significant difference was attributed to the positive effect that finer sand can provide to ECC ductility by lowering the crack-tip matrix toughness. In terms of tensile strength, statistically significant differences were not found due to increasing contents of fly ash. This was attributed to the relatively small differences in strength observed between groups. Details of the statistical analysis are included in the Appendix of this report.

5.2.2. Short-RECS15 Fiber

Figures 14 and 15 present the tensile stress vs. strain curves of all the specimens evaluated for each Short-RECS15 mix design in this study. As it can be observed in Figures 14 and 15, all mixes evaluated exhibited pseudo-strain hardening behavior with significant amounts of deformation capacity. However, as it was the case with Long-RECS15 specimens, material selection (crumb rubber addition, as well as coarse and fine sand utilization) and mix proportioning (increasing contents of fly ash) had a relevant impact on the tensile ductility and strength of the composites.

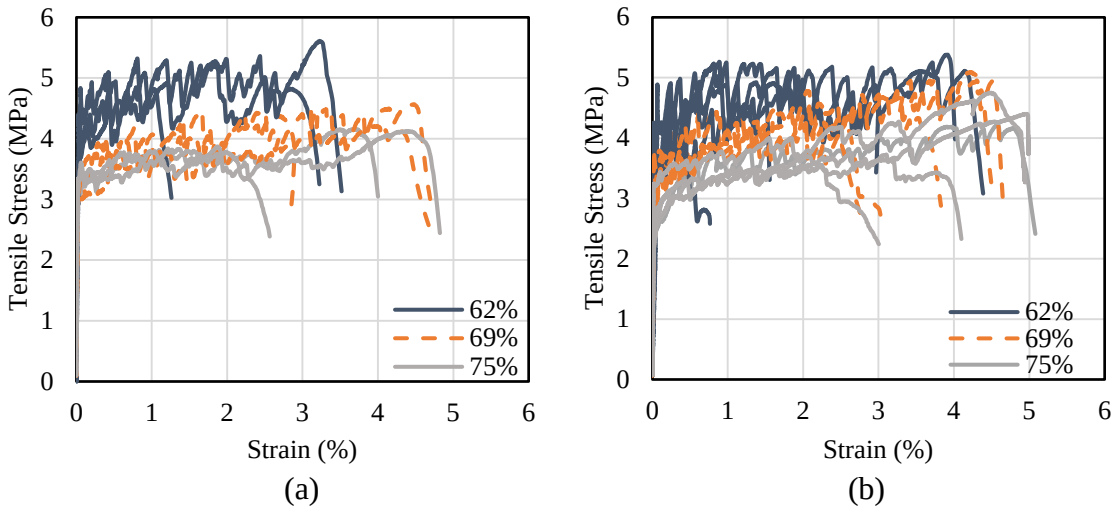

Figure 14. Tensile stress vs. strain curve of regular Short-RECS15 ECC at 62, 69 and 75% cement replacement with fly ash (a) coarse sand and (b) fine sand.

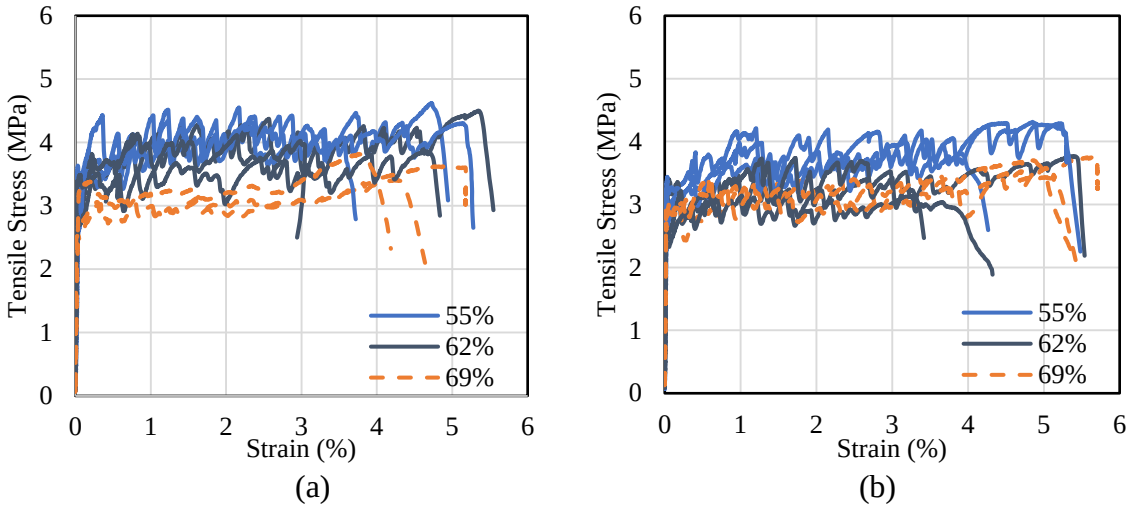

Figure 15. Tensile stress vs. strain curve of crumb rubber Short-RECS15 ECC at 55, 62 and 69% cement replacement with fly ash (a) coarse sand and (b) fine sand.

As shown in Figures 16b and 17b, the partial replacement of sand with crumb rubber (20% by volume) produced important improvements in tensile ductility of the composites. For example, for the mixes with 62% cement replacement with fly ash (M-1.6), the addition of crumb rubber (MR-1.6) produced an increase in tensile ductility from 2.04% to 3.58% (76% improvement) and from 1.72% to 3.44% (100% improvement) for coarse and fine sand specimens, respectively. Furthermore, in the case of mixes with 69% cement replacement with fly ash (M-2.2), the addition of crumb rubber (MR-2.2) produced an increase in tensile ductility from 3.71% to 4.33% (17% improvement) and from 3.12% to 5.18% (66% improvement) for coarse and fine sand specimens, respectively. While the ductility increments were important, a decrease in the tensile strength of the composites was observed due to the addition of crumb rubber as shown in Figures 16a and 17a. In the case of the mixes with a 62% cement replacement with fly ash, the drop in tensile strength was from 5.29 MPa to 4.18 MPa (21%

decrease) and 5.03 MPa to 3.56 MPa (29% decrease) for coarse and fine sand specimens, respectively. Moreover, for the specimens with 69% cement replacement with fly ash, the drop in tensile strength was from 4.40 MPa to 3.62 MPa (18% decrease) and 4.69 MPa to 3.65 MPa (22% decrease) for coarse and fine sand specimens, respectively. The increase in ductility as well as the tensile strength decrease provided by the addition of crumb rubber were attributed to the same phenomenon described above for Long-RECS15 ECC specimens.

Similar to what was observed for Long-RECS15 specimens, the different types of sands evaluated in this study produced minor effects in the tensile strength and tensile ductility of the composites. Differences in tensile strength were found negligible. Furthermore, in contrast to the improvements in ductility observed for Long-RECS15 specimens, the effect of fine sand on the tensile ductility of Short-RECS15 specimens were found to be insignificant.

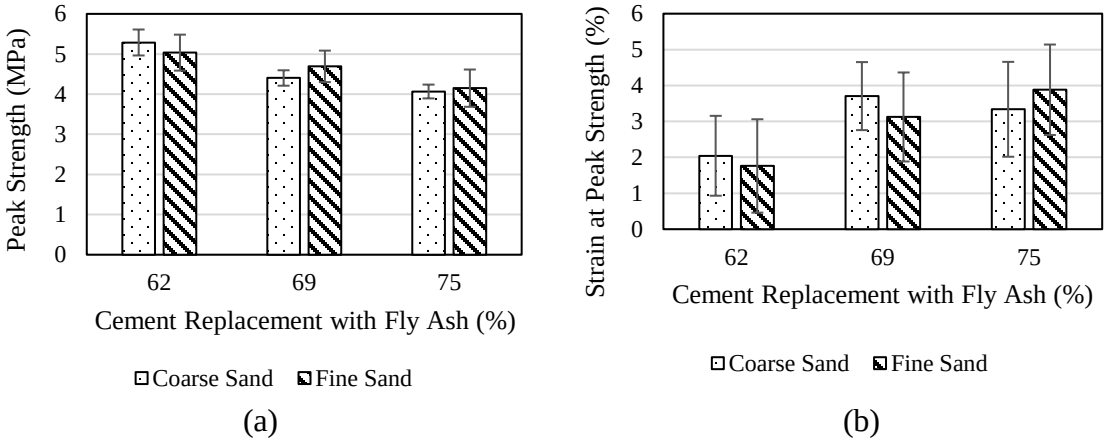

Figure 16. Uniaxial tensile test results of regular Short-RECS15 ECC: (a) peak strength and (b) strain at peak strength.

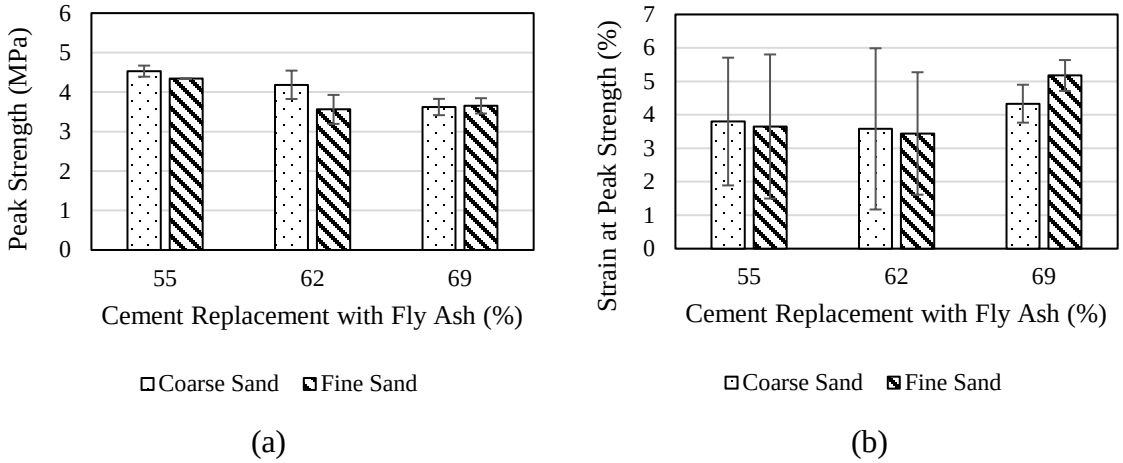

Figure 17. Uniaxial tensile test results of crumb rubber Short-RECS15 ECC: (a) peak strength and (b) strain at peak strength.

As shown in Figures 16 and 17, changes in the mix proportions considered in this study (different levels of cement replacement with fly ash) were also a relevant factor affecting the tensile properties of the ECC materials. Similar to what was observed for Long-RECS15

specimens, the general trend for Short-RECS15 mixes suggested that higher cement replacements with fly ash led to increments in tensile ductility (except for MR-1.6 (62%) compared to MR-1.2 (55%) for coarse and fine sand as well as M-3.0 (75%) compared to M-2.2 (69%) for coarse sand); however, it yielded lower tensile strengths. The improvements in ductility and decrease of tensile strength with increasing contents of fly ash were attributed to the same phenomenon discussed in the Long-RECS15 section above.

In contrast to the observations for Long-RECS15 specimens presented above, statistical analysis conducted according to ANOVA and Tukey-Kramer HSD was not able to demonstrate that increasing contents of fly ash produced statistically significant differences in the tensile ductility for Short-RECS15 mixes. This was attributed to the large variability observed in the tensile ductility of the specimens (likely due to relatively low PSH indexes of some of the ECC materials evaluated) as well as to a more uniform performance in tensile ductility (especially for crumb rubber ECC specimens). In terms of tensile strength, statistical significance was found between M-1.6 (62%) and M-3.0 (75%) for coarse and fine sand specimens. In addition, for crumb rubber ECC specimens statistically significant differences were found between MR-1.2 (55%) compared to MR-2.2 (69%) for coarse and fine and for MR-1.2 (55%) compared to MR-1.6 (62%) for fine sand specimens. Details of the statistical analysis are included in the Appendix.

5.3. Flexural Performance

5.3.1. Long-RECS15 Specimens

Figures 18 and 19 present the flexural stress vs. deformation curves associated to each Long-RECS15 mix design evaluated in this study. As shown in Figures 18 and 19, all the mixes presented significant amounts of deformation capacity typical of ECC materials, exhibiting a concrete like deformation behavior until the first-cracking strength (Figures 20a and 21a) where further deformation led to a dramatic increase in deformation accompanied by an increment in load carrying capacity through multiple cracking plastic deformation of the composite. Yet, material selection (crumb rubber addition, as well as coarse and fine sand utilization) and mix proportioning (increasing contents of fly ash) had a profound impact on the deflection capacity (deflection at peak strength) and modulus of rupture (MOR) of the materials.

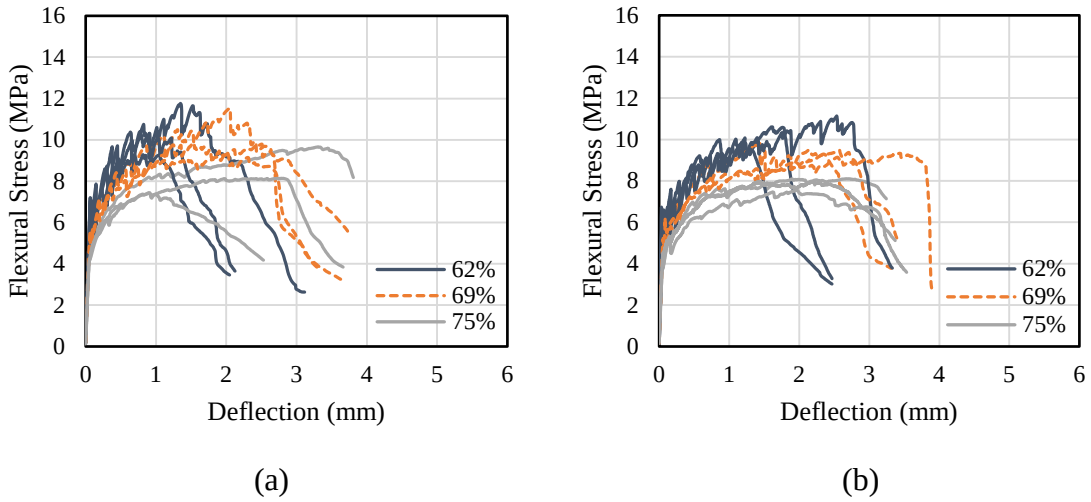

Figure 18. Flexural stress vs. deflection curves of regular Long-RECS15 ECC at 62, 69 and 75% cement replacement with fly ash (a) coarse sand and (b) fine sand.

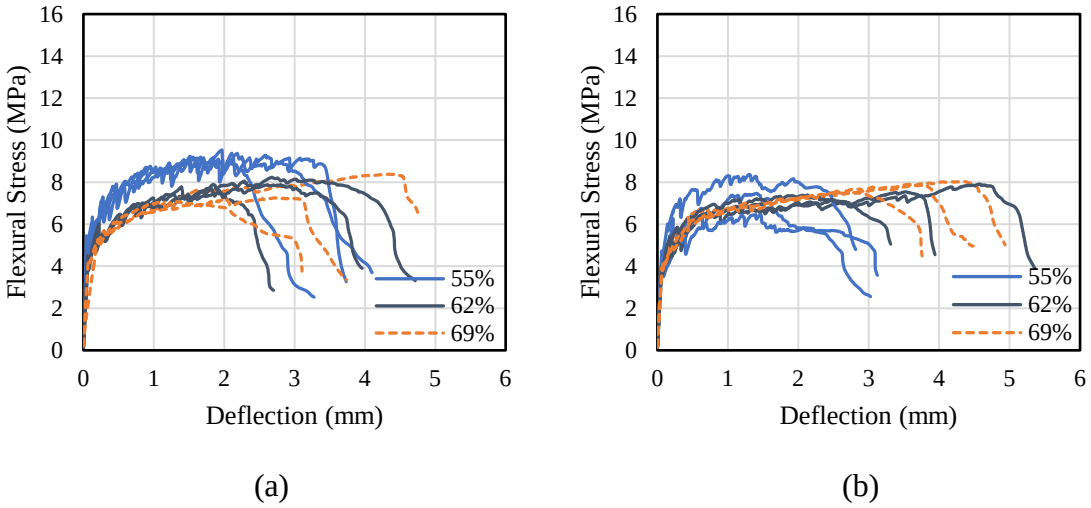

Figure 19. Flexural stress vs. deflection curves of crumb rubber Long-RECS15 ECC at 55, 62 and 69% cement replacement with fly ash (a) coarse sand and (b) fine sand.

As shown in the summarized flexural performance results presented in Figures 20 and 21, the partial replacement of sand with crumb rubber (20% by volume) produced a substantial improvement in deflection capacity of the materials. For mix design M-1.6 (62%) with coarse sand, an improvement from 1.10 mm to 2.34 mm (113% improvement) in deflection capacity was observed when using crumb rubber (MR-1.6). In the same fashion, mix M-1.6 with fine sand presented an improvement from 1.74 mm to 3.39 mm (95% improvement) in deformation capacity when using crumb rubber (MR-1.6). The same trend was observed for M-2.2 (69%) mixes where the addition of crumb rubber (MR-2.2) produced a deflection capacity improvement from 2.04 mm to 2.85 mm (40% improvement) and from 2.46 mm to 3.51 mm (42% improvement) for specimens utilizing coarse and fine sand, respectively.

While the significant improvements in ductility caused by crumb rubber are desirable, a trade-off between ductility and strength (similar to that observed in tensile properties of ECC) was noticeable. M-1.6 (62%) specimens with crumb rubber (MR-1.6) exhibited a reduction in the MOR (flexural strength) from 10.46 MPa to 7.91 MPa (25% decrease) and from 10.59 MPa to 7.62 MPa (28% decrease) for coarse and fine sand specimens, accordingly. Meanwhile, M-2.2 (69%) specimens with crumb rubber (MR-2.2) experienced a modulus of rupture decrease from 10.38 MPa to 7.52 MPa (28% decrease) and from 9.57 MPa to 7.83 MPa (18% decrease) for coarse and fine sand specimens, respectively. It is important to notice that, while the reduction in modulus of rupture was significant, the increases in ductility were much superior.

The effect of crumb rubber addition on the flexural performance of ECC is mainly the result of the effects of crumb rubber in the tensile properties of ECC. This is the case, since flexural failure in concrete materials are controlled by the tensile failure mode *(23)*. As reported in the uniaxial tensile test section of this report, crumb rubber addition enhanced the PSH energy index (J'_b/J_{tip}) leading to an increase in tensile ductility; thus, enhancing deflection capacity of the beam. Moreover, the implementation of crumb rubber produced a decrease in the fiber bridging capacity σ_0 leading to a decrease in the tensile strength of the material; consequently, producing the observed decrease in the modulus of rupture of ECC when implementing crumb rubber.

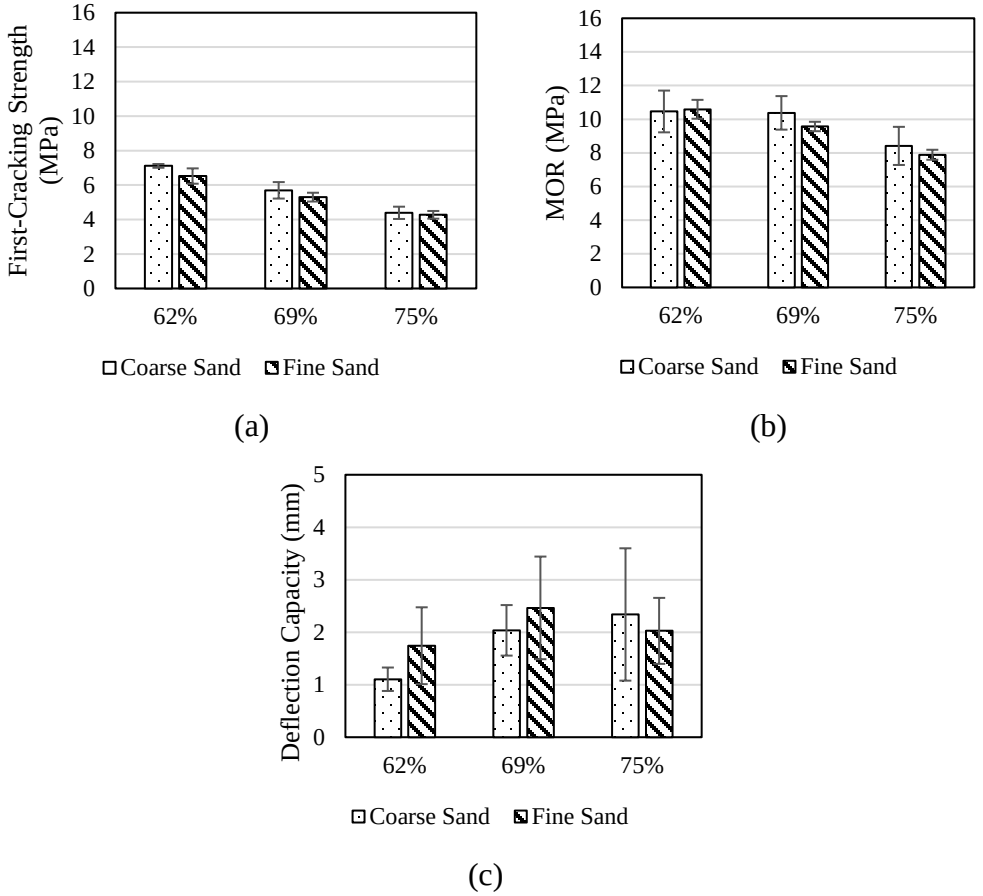

Figure 20. Flexural performance of regular Long-RECS15 ECC: (a) first-cracking strength, (b) modulus of rupture, and (c) deflection capacity.

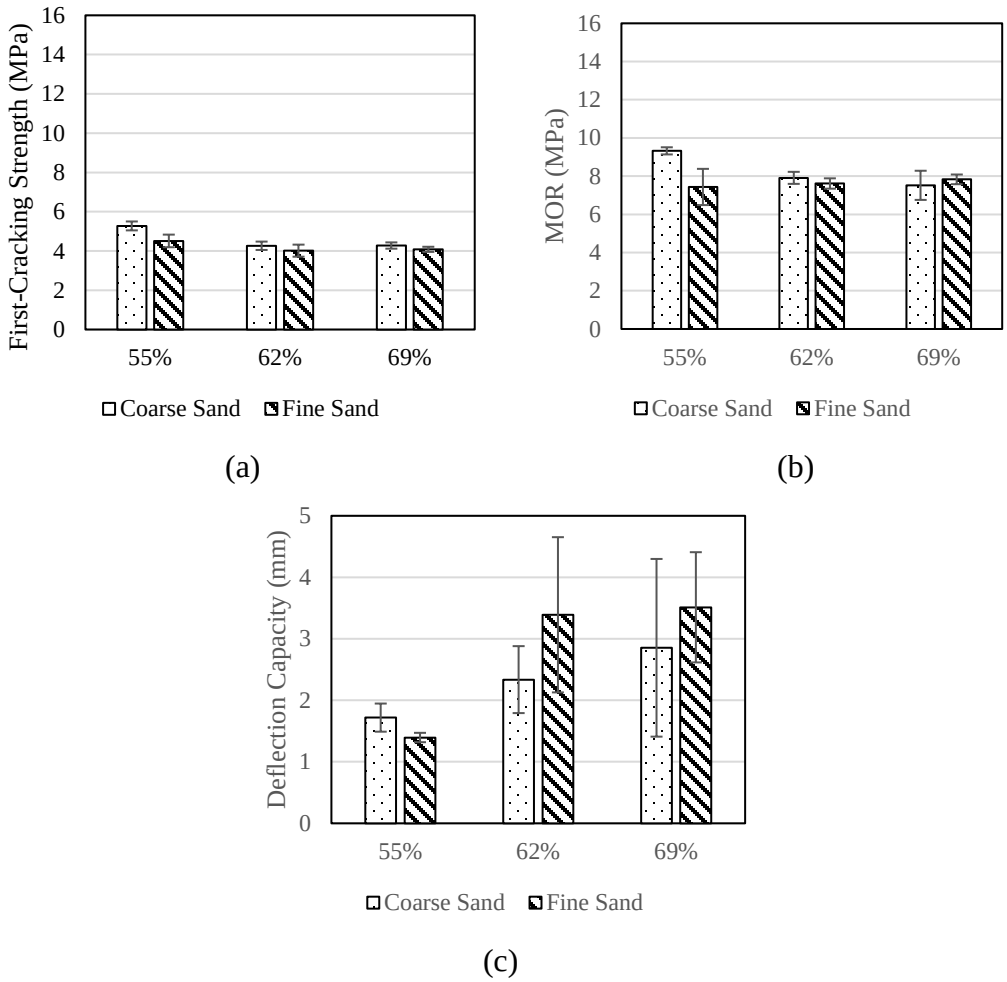

Figure 21. Flexural performance of crumb rubber Long-RECS15 ECC: (a) first-cracking strength, (b) modulus of rupture, and (c) deflection capacity.

The use of different types of sands produced minor effects on the flexural performance of ECC specimens. Using finer sand produced some enhancements in deflection capacity of M-1.6 (62%), M2.2 (69%), MR-1.6 (62%) and MR-2.2 (69%) mix designs likely due to the reduction in matrix fracture toughness produced by the finer sand. However, changes in strength due to the utilization of different types of sands were negligible.

Changes in the mix proportions evaluated in this study influenced the flexural performance of ECC materials. Higher cement replacements with fly ash led to increases in ductility (except for M-3.0 (75%) compared to M-2.2 (69%) for fine sand specimens). However, as in the case of crumb rubber addition, a trade-off between ductility and strength was evident. Increases in deflection capacity of up to 113% (1.10 mm to 2.34 mm from 62% to 75% cement replacement) and 41% (1.74 mm to 2.46 mm from 62% to 69% cement replacement) for coarse and fine sand ECC specimens were obtained by increasing fly ash contents, respectively. On the other hand, a decrease in flexural strength of up to 20% (10.46 MPa to 8.41 MPa from 62% to 75% cement replacement) and 26% (10.59 MPa to 7.89 MPa from 62% to 75% cement replacement) was observed for coarse and fine sand specimens, accordingly. In the case of crumb rubber

ECC, the increases in deflection capacity were up to 66% (1.72 mm to 2.85 mm from 55% to 69% cement replacement) for coarse sand specimens and 151% (1.40 mm to 3.51 mm from 55% to 69% cement replacement) for fine sand specimens. However, flexural strength was slightly affected by increasing the content of fly ash, with a decrease of up to 19% (9.32 MPa to 7.52 MPa from 55% to 69% cement replacement) for coarse sand specimens and negligible changes for fine sand specimens throughout all the levels of cement replacement with fly ash. As in the case of crumb rubber addition, the effects of increasing contents of fly ash on the flexural performance of ECC materials was attributed to its effects on the tensile properties of ECC (as described in the uniaxial tensile test section), which controlled the failure of the beam specimen.

Statistical analysis was conducted to determine potential statistically significant differences among flexural properties of the different mix designs proposed due to changes in mix proportions or use of different sands. The statistical analysis conducted (according to ANOVA and Tukey-Kramer HSD) showed that for regular ECC specimens with fine sand the decrease in MOR due to increasing fly ash content from 62% to 75% was statistically significant. On the other hand, the decrease in MOR due to the increase in fly ash content from 55% to 69% for crumb rubber ECC specimens with coarse sand was also found to be statistically significant. Surprisingly, statistical significance in MOR was also found for crumb rubber ECC specimens with 55% cement replacement with fly ash due to the use of different types of sand. In terms of deflection capacity, no statistically significant differences were found. Details of the statistical analysis are included in the Appendix of this report.

It is important to notice that all mixes evaluated exhibited a modulus of rupture exceedingly superior than that of normal strength concrete (approximately 4.5 MPa) as well as a dramatic increase in the deflection capacity from about 0.05 mm at the first-cracking strength (which would approximate the deflection capacity of concrete) up to 3.51 mm for MR-2.2 specimens with fine sand (more than 70 times the deformation capacity).

5.3.2. Short-RECS15 Specimens

All tests conducted in this study (compressive test, uniaxial tensile test and flexural test) were performed after 28 days of curing. However, in order to gain insight on the long-term performance of the evaluated ECC mix designs, Short-RECS15 beam specimens were tested after 70 days of curing. Figures 22 and 23 present the flexural stress vs. deformation curves for each Short-RECS15 mix design evaluated in this study. As shown in Figures 22 and 23, all the mixes presented significant amounts of deformation capacity typical of ECC materials, exhibiting pseudo strain-hardening phenomenon. Yet, as observed for Long-RECS15 mix designs, materials selection (crumb rubber addition, as well as coarse and fine sand utilization) and mix proportioning (increasing contents of fly ash) influenced the flexural performance of the materials.

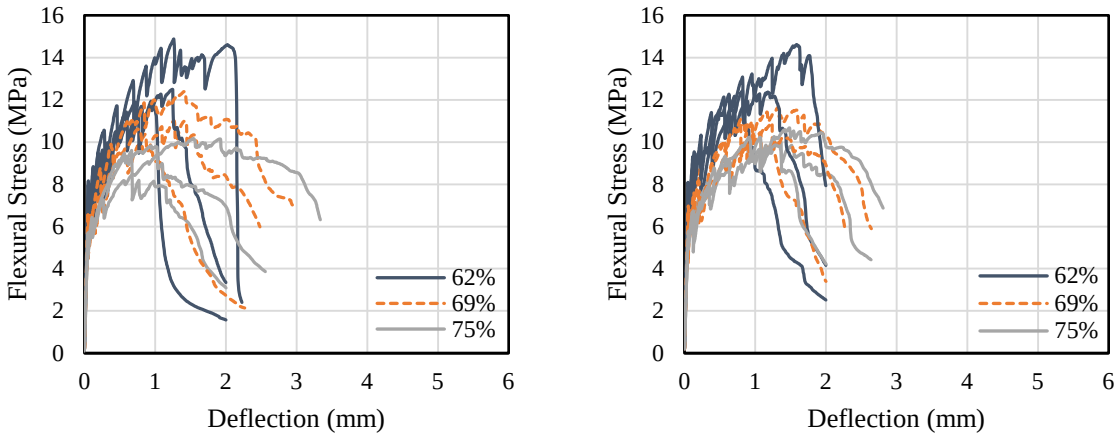

Figure 22. Flexural stress vs. deflection curves of regular Short-RECS15 ECC at 62, 69 and 75% cement replacement with fly ash (a) coarse sand and (b) fine sand.

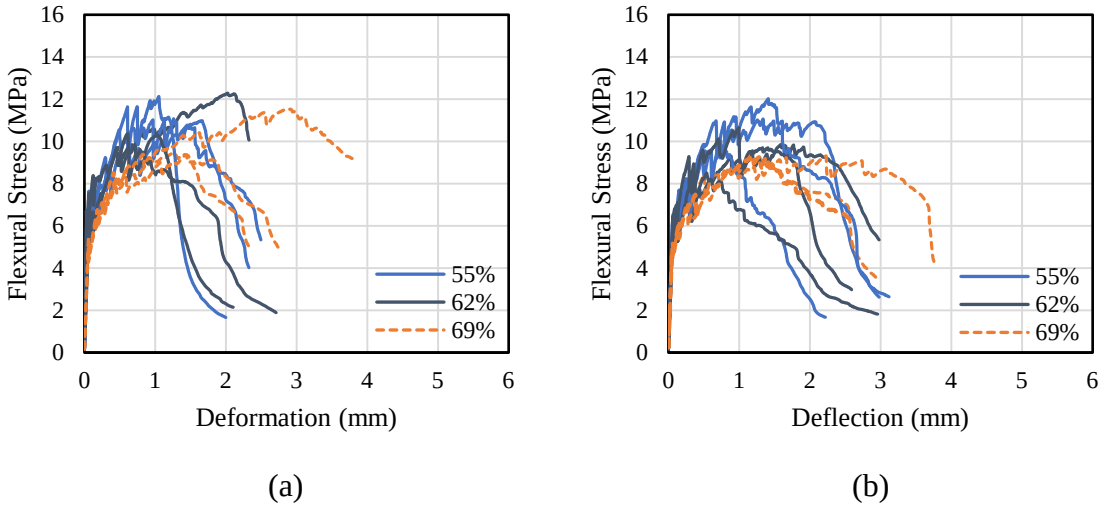

Figure 23. Flexural stress vs. deflection curves of crumb rubber Short-RECS15 ECC at 55, 62 and 69% cement replacement with fly ash (a) coarse sand and (b) fine sand.

As shown in the summarized flexural performance results presented in Figures 24 and 25, the partial replacement of sand with crumb rubber (20% by volume) produced an improvement in deflection capacity of ECCs. For M-2.2 (69%) mixes, the addition of crumb rubber (MR-2.2) caused a deflection capacity improvement from 1.15 mm to 1.86 mm (62% improvement) and from 1.07 mm to 1.56 mm (45% improvement) for specimens using coarse and fine sand, respectively. However, for coarse and fine sand M-1.6 (62%) mix designs, the deflection capacity improvements were negligible when using crumb rubber (MR-1.6).

While the possibility of improving deflection capacity by using crumb rubber is desirable, a decrease in MOR due to crumb rubber addition was noticed. M-1.6 (62%) specimens with crumb rubber (MR-1.6) exhibited a reduction in the modulus of rupture from 13.08 MPa to 10.82 MPa (17% decrease) and from 13.07 MPa to 9.67 MPa (26% decrease) for coarse and fine sand specimens, accordingly. Meanwhile, M-2.2 (69%) specimens with crumb rubber

(MR-2.2) experienced a modulus of rupture decrease from 11.34 MPa to 10.12 MPa (11% decrease) and from 11.06 MPa to 9.29 MPa (16% decrease) for coarse and fine sand specimens, respectively. The effect of crumb rubber on the flexural performance of Short-RECS15 ECC is attributed to the same phenomenon discussed for Long-RECS15 ECC specimens above. It is important to notice, that similar to what was observed for Long-RECS15 specimens, the use of different types of sands had small effects on the flexural performance of Short-RECS15 ECC specimens.

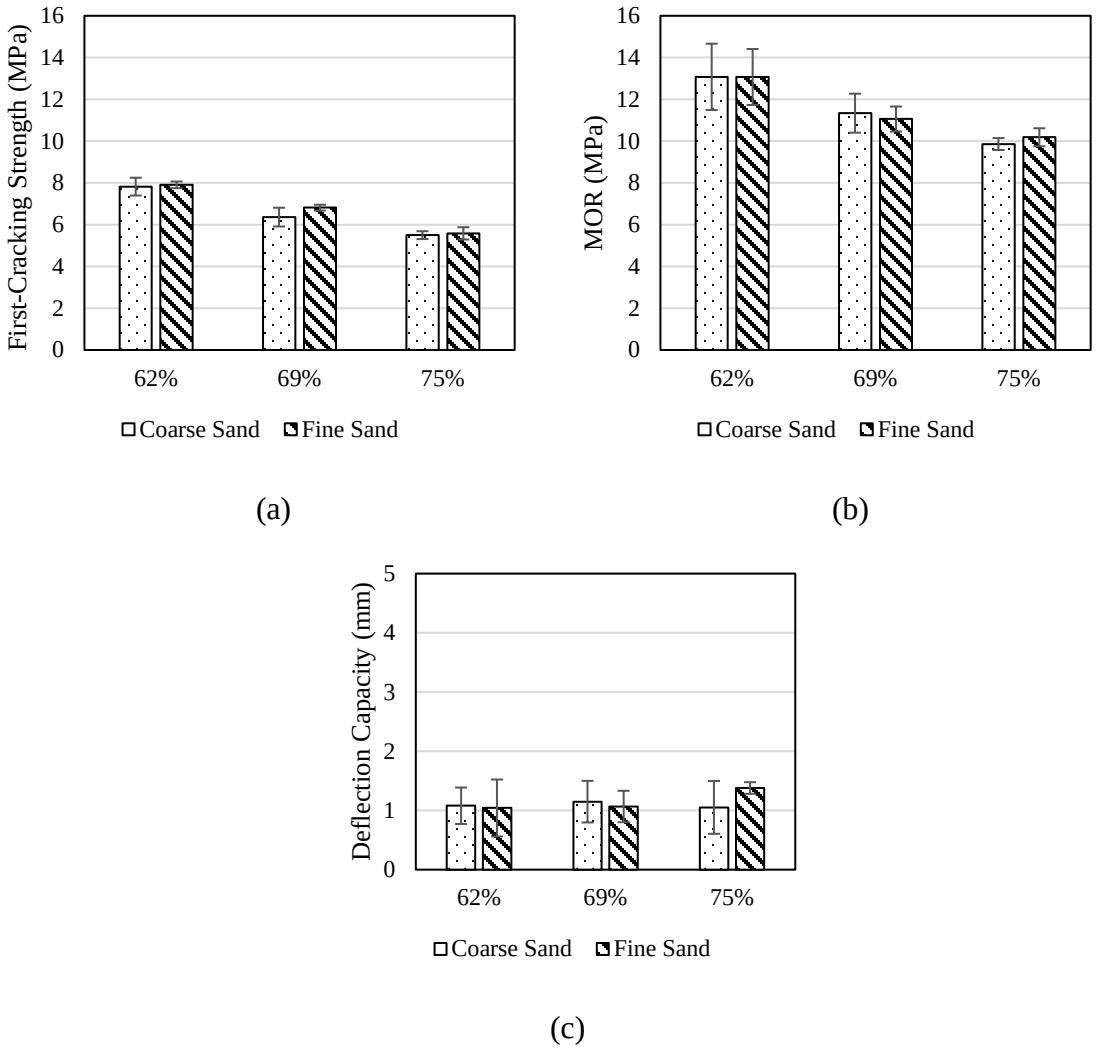

Figure 24. Flexural performance of regular Short-RECS15 ECC: (a) first-cracking strength, (b) modulus of rupture, and (c) deflection capacity.

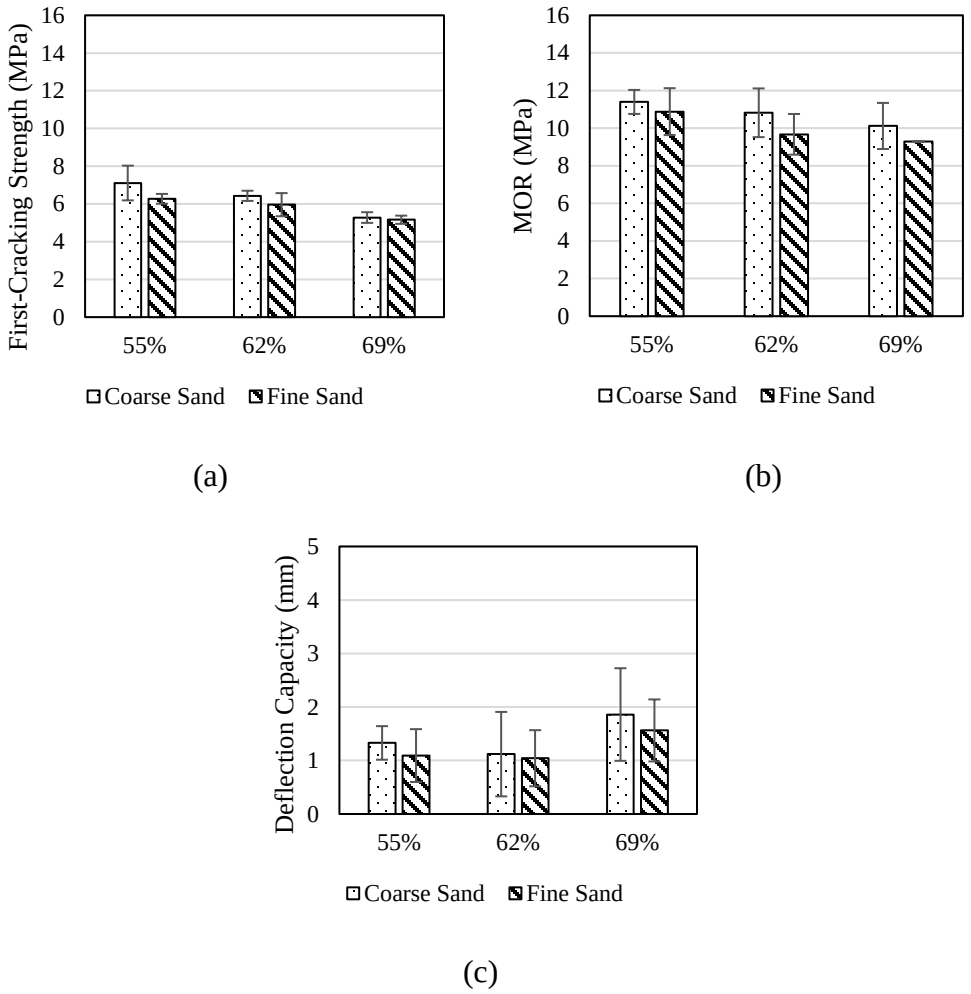

Figure 25. Flexural performance of crumb rubber Short-RECS15 ECC: (a) first-cracking strength, (b) modulus of rupture, and (c) deflection capacity.

In terms of the mix proportions evaluated in this study, modification of cement replacement with fly ash produced some noticeable effects on the flexural performance of Short-RECS15 ECC materials. Higher cement replacements with fly ash tended to increase ductility; yet, the effect of increasing contents of fly ash in ductility for Short-RECS15 specimens was reduced as compared with Long-RECS15 specimens (likely due to the longer curing time). Increments in deflection capacity of up to 7% (1.08 mm to 1.15 mm from 62% to 69% cement replacement) and 33% (1.04 mm to 1.38 mm from 62% to 75% cement replacement) for coarse and fine sand ECC specimens were obtained by increasing fly ash contents, respectively.

On the other hand, a decrease in flexural strength of up to 25% (13.08 MPa to 9.86 MPa from 62% to 75% cement replacement) and 22% (13.07 MPa to 10.18 MPa from 62% to 75% cement replacement) was observed for coarse and fine sand specimens, accordingly. In the case of crumb rubber ECC, the increases in deflection capacity were up to 40% (1.33 mm to 1.86 mm from 55% to 69% cement replacement) for coarse sand specimens and 43% (1.09 mm to 1.56 mm from 55% to 69% cement replacement) for fine sand specimens. However, flexural strength was marginally affected by increasing contents in fly ash, with a decrease of up to

11% (11.40 MPa to 10.12 MPa from 55% to 69% cement replacement) for coarse sand specimens and 15% (10.88 MPa to 9.29 MPa from 55% to 69% cement replacement) for fine sand. The effects of increasing contents of fly ash on the flexural performance of ECC materials was attributed to the same phenomenon discussed for Long-RECS15 ECC.

Statistical analysis was conducted to determine potential statistically significant differences among flexural properties of the different mix designs proposed due to changes in mix proportions or utilization of different sands. The statistical was conducted according to ANOVA and Tukey-Kramer HSD. However, no statistically significant differences were found. Details of the statistical analysis are included in the Appendix of this report.

It is important to notice that all mixes evaluated exhibited a modulus of rupture much superior than that of normal strength concrete (approximately 4.5 MPa) as well as a dramatic increase in the deflection capacity from about 0.05 mm at the first-cracking strength (which would approximate the deflection capacity of concrete) up to 1.86 mm for MR-2.2 specimens with coarse sand (more than 37 times the deformation capacity).

5.4. Characterization of ECC Cracking

Cracks in concrete allow detrimental substances to penetrate the structure and cause durability issues. However, tight crack widths (smaller than 200 μm) in concrete materials have been shown to produce transport properties (water permeability and chloride diffusion) almost equivalent to those of uncracked concrete *(2,24)*. Unlike regular concrete, ECC exhibits high ductility by the formation of multiple tight microcracks (typically between 60-100 μm). In contrast to typical cracks formed in regular concrete (in the order of millimeters in size), the formation of tight microcracks are beneficial to durability of the material and structure. Figure 26 presents the average residual crack width observed in dog-bone shaped specimens after being subjected to the uniaxial tensile test. The residual average crack width was quantified by measuring the size of each crack present in each dog-bone shape specimens. Three replicas per mix design were investigated under the light microscope.

5.4.1. Long-RECS15 Specimens

As shown in Figure 26, cracks formed in Long-RECS15 mix designs were tight and did not exceeded an average width of 68 μm for any given mix. Furthermore, increasing contents of fly ash presented a clear tendency to benefit the formation of tighter cracks for regular and crumb rubber ECC (except for MR1.2 (55%) for coarse sand specimens). Furthermore, it was clearly observed that the implementation of crumb rubber produced additional crack tightness. For instance, M-1.6 (62%) specimens experienced a reduction in average residual crack width from 67.7 μm to 40.6 μm for coarse sand specimens and from 52.5 μm to 46.9 μm for fine sand when implementing crumb rubber (MR-1.6).

The addition of crumb rubber produced a decrease in crack size for M-2.2 (69%) specimens from 38.2 μm to 29.5 μm and from 43.7 μm to 42.3 μm for coarse and fine sand, respectively. As previously discussed, increasing contents of fly ash as well as crumb rubber addition produced an increase in the PSH energy index. In turn, this translates into a more robust multiple cracking behavior yielding tighter cracks as well as an enhanced ductility of the composite. In addition, it is important to mention that cracks under 50 μm in width have been

reported to significantly benefit from the autogenous healing of cementitious materials; thus providing robust self-healing ability to the material *(25)*.

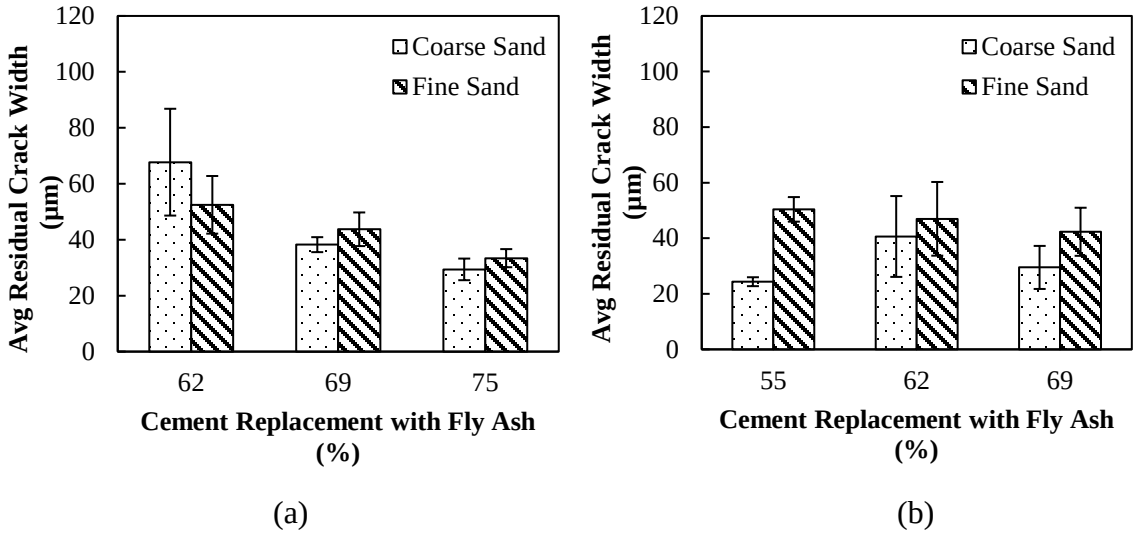

Figure 26. Average residual crack width of Long-RECS15 ECC: (a) regular ECC and (b) crumb rubber ECC.

5.4.2. Short-RECS15 Specimens

The crack analysis results for Short-RECS15 specimens showed that the average residual crack widths did not exceed 94 μm wide for any mix design evaluated. Furthermore, similar to what was observed for Long-RECS15 specimens, increasing contents of fly ash presented a clear tendency to benefit the formation of tighter cracks for regular and crumb rubber ECC as shown in Figure 27. In addition, the implementation of crumb rubber produced additional crack tightness. For instance, M-1.6 (62%) specimens experienced a reduction in average residual crack width from 68.4 μm to 60.9 μm for coarse sand specimens and from 93.5 μm to 54.6 μm for fine sand specimens when using crumb rubber (MR-1.6). Moreover, the addition of crumb rubber produced a decrease in crack size for M-2.2 (69%) specimens from 64.2 μm to 53.1 μm and from 83.8 μm to 49.3 μm for coarse and fine sand, respectively. This behavior is explained by the same phenomena discussed for Long-RECS15 specimens. Moreover, it is important to mention that the size of cracks present was larger than those observed in Long-RECS15 specimens. However, samples with high fly ash content or crumb rubber could potentially benefit from a robust self-healing ability.

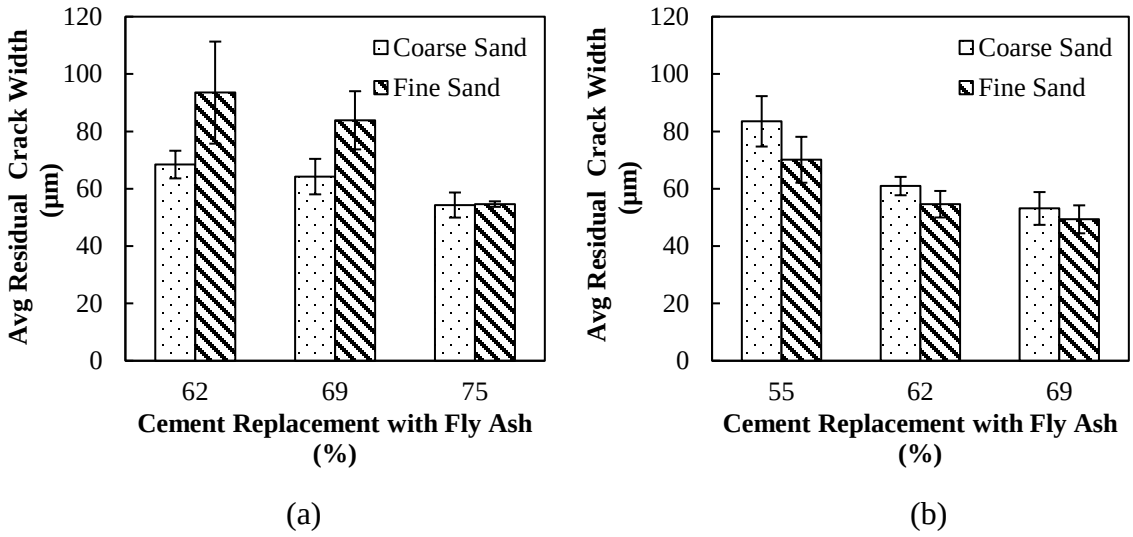

Figure 27. Average residual crack width of Short-RECS15 ECC: (a) regular ECC and (b) crumb rubber ECC.

5.5. Cost-Analysis and Feasibility

A cost analysis was performed to determine the feasibility of implementing ECC as a novel pavement material for the future of transportation infrastructure. As shown in Tables 5 and 6, several of the ECC materials evaluated in this study possess superior properties, which make them attractive for transportation infrastructure application. However, its cost compared to regular concrete is high (2.8 to 4.1 times as shown in Tables 5 and 6). While the high cost of ECC could suggest that utilizing these materials is not feasible, it can be greatly misleading to compare regular concrete and ECC solely on their cost without taking into consideration the profound implications of ECC properties on pavement design, construction, and performance.

Currently, limited information exists on pavement design with ECC. However, Qian and Li proposed a simplified design chart for ECC pavements based on the integration of an experimental study of fatigue performance of ECC and FEM analysis *(26)*. It is important to notice that the design chart is based on a 3.6 m by 6.1 m slab and does not account for the plastic behavior of ECC; thus, being conservative. In addition, the design chart is limited to ECC materials similar to the one utilized to develop the chart. Yet, as shown in Table 7, mix design M-2.2 (Short-C) closely replicates the properties of the ECC material utilized to develop the design chart. Interestingly, from all the materials evaluated in this study, M-2.2 (Short-C) mix design was also one of the most promising mix designs due to its properties and cost (Table 5). M-2.2 (Short-C) exhibited a compressive strength of 40.3 MPa (higher than regular concrete), a modulus of rupture of 11.3 MPa (more than 2 times that of regular concrete), a tensile ductility (ε_{tu}) of 3.7% (370 times that of regular concrete) and possessed one of the lowest costs (about 2.8 times that of typical concrete). For these reasons, M-2.2 (Short-C) was selected for the cost analysis.

Table 5. Properties and cost of regular ECC mix designs.

Mix ID	f 'c (MPa)	σtu (MPa)	εtu (%)	MOR (MPa)	CW (µm)	Cost
M-1.6 (Long-C)	39.5	4.8	0.8	10.5	67.7	4.0
M-2.2 (Long-C)	31.3	4.6	1.7	10.4	38.2	3.9
M-3.0 (Long-C)	23.9	3.8	3.6	8.4	29.4	3.9
M-1.6 (Long-F)	34.6	4.7	1.2	10.6	52.5	4.0
M-2.2 (Long-F)	27.6	4.5	2.8	9.6	43.7	3.9
M-3.0 (Long-F)	20.8	3.8	3.0	7.9	33.4	3.9
M-1.6 (Short-C)	48.3	5.3	2.0	13.1	68.4	2.9
M-2.2 (Short-C)	40.3	4.4	3.7	11.3	64.2	2.8
M-3.0 (Short-C)	36.0	4.1	3.3	9.9	54.3	2.8
M-1.6 (Short-F)	49.0	5.0	1.8	13.1	93.5	2.9
M-2.2 (Short-F)	42.2	4.7	3.1	11.1	83.9	2.8
M-3.0 (Short-F)	34.5	4.2	3.9	10.2	54.6	2.8

Table 6. Properties and cost of crumb rubber ECC mix designs.

Mix ID	f 'c (MPa)	σtu (MPa)	εtu (%)	MOR (MPa)	CW (µm)	Cost
MR-1.2 (Long-C)	23.0	4.0	1.6	9.3	24.4	4.1
MR-1.6 (Long-C)	18.2	3.5	4.1	7.9	40.6	4.0
MR-2.2 (Long-C)	16.2	3.4	3.5	7.5	29.5	3.9
MR-1.2 (Long-F)	20.3	4.1	3.5	7.4	50.4	4.1
MR-1.6 (Long-F)	17.3	3.6	3.5	7.6	47.0	4.0
MR-2.2 (Long-F)	15.1	3.5	3.8	7.8	42.2	3.9
MR-1.2 (Short-C)	32.8	4.5	3.8	11.4	83.5	3.0
MR-1.6 (Short-C)	32.5	4.2	3.6	10.8	60.9	2.9
MR-2.2 (Short-C)	26.0	3.6	4.3	10.1	53.1	2.8
MR-1.2 (Short-F)	32.9	4.3	3.7	10.9	70.1	3.0
MR-1.6 (Short-F)	28.8	3.6	3.4	9.7	54.6	2.9
MR-2.2 (Short-F)	27.8	3.7	5.2	9.3	49.3	2.8

As shown in Figure 28, due to the enhanced properties of ECC in contrast to regular concrete a thickness ratio exists between ECC and regular concrete for the same performance (cycles to failure). Assuming a rigid pavement that is designed for a total of 10 million cycles (i.e., 10 million ESALs), we can use the chart and obtain the thickness ratio between ECC and concrete. For 10 million cycles the thickness ratio is approximately 2.25, meaning that for the same performance, the ECC pavement can be 2.25 times thinner than a regular concrete pavement.

If we factor in the thickness ratio in the cost calculations and to account for the difference in performance between concrete and ECC over the life cycle of the pavement, the cost changes drastically. The 2.8 cost factor between the proposed ECC mix design and regular concrete becomes a 1.24 factor, meaning that the true increase in material cost would only be 24%. While this still places ECC as a more expensive alternative, other important factors need to be taken into consideration. Due to the exceptional ductility of ECC materials, ECC pavements can be constructed without joints *(24)*. In turn, this can produce huge cost savings in the construction of rigid pavements making a 24% increase in materials cost negligible. In addition, due to the possibility of jointless pavements with ECC, it is expected that the repair and maintenance cost of ECC pavements would be much lower than that of typical jointed concrete pavements. For instance, commonly observed distresses in rigid pavements such as

joint faulting, joint spalling and corner breaks would not exist in ECC pavements; thus, producing significant cost savings in repair and maintenance over the life cycle of the pavement structure. In addition, the ability to construct rigid pavements without joints, would provide an improvement in ride quality; thus, benefiting the users.

Table 7. Design chart materials.

Material	f 'c (MPa)	σtu (MPa)	εtu (%)	MOR (MPa)
Concrete (Qian and Li)	27.0	-	0.01	4.6
ECC (Qian and Li)	37.5	4.9	3.7	11.1
M-2.2 (Short-C)	40.3	4.4	3.7	11.3

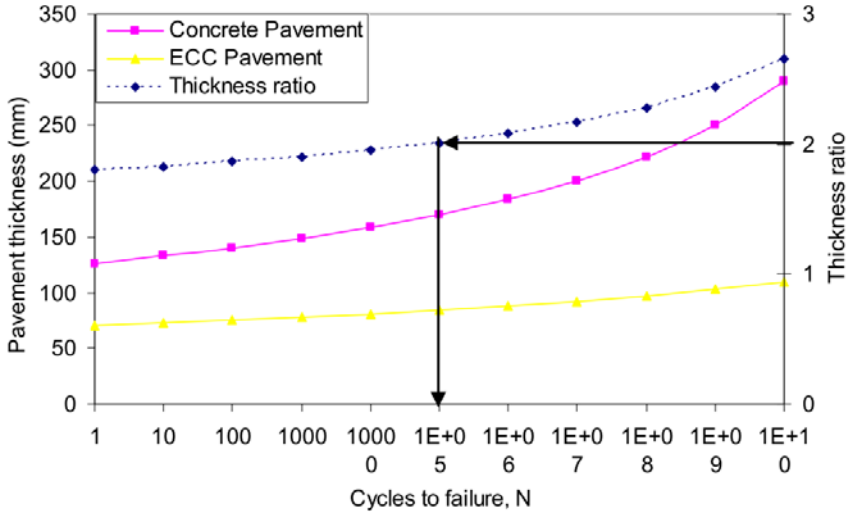

Figure 28. Pavement thickness vs. cycles to failure for concrete and ECC *(26)*.

6. CONCLUSIONS

ECC materials at different levels of cost and performance were successfully developed using locally available ingredients in Region 6. The main effects studied were the impacts of materials selection (type of sand and crumb rubber implementation) and mix proportioning (increasing contents of fly ash) on the mechanical properties of the materials. After analysis of the experimental data, the following conclusions can be drawn:

- Increasing contents of cement replacement with fly ash caused lower compressive strengths in ECC materials, proportionally. This behavior was attributed to the high content of fly ash and low water to binder ratio (W/B=0.27) used in ECC mixes, which likely limited the secondary hydration reaction of fly ash making it to partially act as a filler. Furthermore, the most important factor influencing compressive strength of ECC was the addition of crumb rubber. Due to the defect-like behavior of crumb rubber in the cementitious matrix, its implementation in ECC mixes caused a significant reduction in compressive strength. On the other hand, the different types of sands utilized in this study produced a minor impact on the compressive strengths of the ECC materials investigated.
- Tensile ductility of ECC specimens was dramatically improved by the implementation of crumb rubber. However, the tensile strengths of the materials were negatively affected (yet, to a lesser degree). Improvements in tensile ductility due to crumb rubber addition (20% replacement of sand by volume) were of up to 434% and 100% for Long-RECS15 and Short-RECS15 specimens, respectively. Meanwhile, tensile strengths decreased up to 26% and 29% for Long-RECS15 and Short-RECS15 specimens, respectively. Similar to the effect of crumb rubber in ECC tensile properties, increasing contents of fly ash favored ductility of the composites; yet, produced lower tensile strengths (both of these effects to a lesser degree than crumb rubber addition). Furthermore, the utilization of the different types of sands explored in this study produced minor impacts on the tensile properties of the materials. The tradeoff between ductility and strength observed due to crumb rubber addition and increasing contents of fly ash was associated to the increase in the PSH energy index (J'_b/J_{tip}) and the decrease in the fiber bridging capacity (σ_0) provided by crumb rubber and fly ash.
- The deflection capacity of ECC beams was significantly improved by the implementation of crumb rubber (up to 113% and 62% for Long-RECS15 and Short-RECS15, respectively). However, flexural strength was negatively affected (up to 28% and 26% for Long-RECS15 and Short-RECS15 specimens, respectively). In addition, a similar trade-off between deflection capacity and strength was observed by increasing contents of fly ash of the ECC mix designs; yet, to a lesser degree than when crumb rubber was added. Since flexural failure in cementitious materials is controlled by the tensile failure mode of the material, the phenomena observed due to crumb rubber addition and fly ash content increments in ECC beam specimens was attributed to the effect of crumb rubber and fly ash in the tensile properties of ECC.
- The average residual crack width did not exceed 68 μm and 94 μm in width for Long-RECS15 and Short-RECS15 mix designs, respectively. The thigh crack width reported suggest that the prepared ECC materials have an excellent durability potential.

- The properties of the ECC materials produced were exceedingly superior to that of regular concrete materials. For instance, one of the best performing mix design in terms of mechanical properties and cost, M-2.2 (Short-C), exhibited a compressive strength of 40.3 MPa (greater than normal strength concrete), a tensile ductility of 3.7% (370 times greater than concrete), a modulus of rupture of 11.3 MPa (more than 2 time greater than regular concrete), and a controlled average crack size of less than 65 μm (after subjecting it to its ultimate deformation capacity).
- Based on the cost analysis, it was concluded that ECC materials are promising for the future of transportation infrastructure. However, research should be directed towards developing and validating (by full-scale tests) robust performance prediction models for ECC pavements. In addition, in depth, studies should be conducted to investigate the impact of jointless rigid pavements in the cost of construction as well as in repair and maintenance cost, so that highly accurate lifecycle cost assessments of ECC pavements can be conducted.

7. RECOMMENDATIONS

Research should be directed towards the development and validation of robust performance prediction models for the design of ECC pavements. To this end, in depth studies should be conducted on the fatigue performance of ECC materials as well as on the response of ECC materials to traffic loading. In addition, full-scale testing of ECC materials should be performed to validate and/or calibrate the developed performance prediction models. Furthermore, research should be conducted to investigate the impact of jointless rigid pavements with ECC in the cost of construction, repair, and maintenance of pavements.

REFERENCES

1. M. L. and V. C. Li, “Influence of Material Ductility on Performance of Concrete Repair,” *Aci Mater. J.*, pp. 419–428, 2009.

2. V. C. Li, “Engineered Cementitious Composites (ECC) – Material , Structural , and Durability Performance,” *Concr. Constr. Eng. Handb.*, p. 78, 2008.

3. M. Sahmaran, M. Lachemi, K. M. A. Hossain, R. Ranade, and V. C. Li, “Influence of aggregate type and size on ductility and mechanical properties of engineered cementitious composites,” *ACI Mater. J.*, vol. 106, no. 3, pp. 308–316, 2009.

4. H. Ma, S. Qian, Z. Zhang, Z. Lin, and V. C. Li, “Tailoring Engineered Cementitious Composites with local ingredients,” *Constr. Build. Mater.*, vol. 101, pp. 584–595, 2015.

5. V. C. Li, S. Wang, and C. Wu, “Tensile strain-hardening behavior of polyvinyl alcohol engineered cementitious composite (PVA-ECC),” *Mater. J.*, vol. 98, no. 6, pp. 483–492, 2001.

6. M. Sahmaran and V. C. Li, “Suppressing Alkali-Silica Expansion,” *Concr. Int.*, pp. 47–52, 2016.

7. H. Liu, Q. Zhang, V. Li, H. Su, and C. Gu, “Durability study on engineered cementitious composites (ECC) under sulfate and chloride environment,” *Constr. Build. Mater.*, vol. 133, pp. 171–181, 2017.

8. Y. Yang, M. D. Lepech, E. H. Yang, and V. C. Li, “Autogenous healing of engineered cementitious composites under wet-dry cycles,” *Cem. Concr. Res.*, vol. 39, no. 5, pp. 382–390, 2009.

9. M. Şahmaran, G. Yildirim, R. Noori, E. Ozbay, and M. Lachemi, “Repeatability and Pervasiveness of Self-Healing in Engineered Cementitious Composites,” *ACI Mater. J.*, vol. 112, no. 4, pp. 513–522, 2015.

10. V. C. Li, “On engineered cementitious composites (ECC). A review of the material and its applications,” *J. Adv. Concr. Technol.*, vol. 1, no. 3, pp. 215–230, 2003.

11. S. Qian, M. D. Lepech, Y. Y. Kim, and V. C. Li, “Introduction of transition zone design for bridge deck link slabs using ductile concrete,” *ACI Struct. J.*, vol. 106, no. 1, pp. 96–105, 2009.

12. V. C. Li, “From Micromechanics Engineering Design for Compo- of Cementitious Engineering,” *JSCE J. Struct. Mech. Earthq. Eng.*, vol. 471, no. I-24, p. 37s–48s, 1993.

13. V. C. Li, C. Wu, S. Wang, A. Ogawa, and T. Saito, “Interface tailoring for strain-hardening polyvinyl alcohol-engineered cementitious composite (PVA-ECC),” *ACI Mater. J.*, vol. 99, no. 5, pp. 463–472, 2002.

14. Z. Pan, C. Wu, J. Liu, W. Wang, and J. Liu, “Study on mechanical properties of cost-effective polyvinyl alcohol engineered cementitious composites (PVA-ECC),” *Constr. Build. Mater.*, vol. 78, pp. 397–404, 2015.

15. G. Fischer and V. C. Li, “Effect of fiber reinforcement on the response of structural

members," *Eng. Fract. Mech.*, vol. 74, no. 1–2, pp. 258–272, 2007.

16. E. Yang, "Designing Added Functions in Engineered Cementitious Composites," p. 276, 2008.

17. M. Li and V. C. Li, "Rheology, fiber dispersion, and robust properties of Engineered Cementitious Composites," *Mater. Struct.*, vol. 46, no. 3, pp. 405–420, 2013.

18. ASTM Standard C 192, *Standard Practice for Making and Curing Concrete Test Specimens in the Laboratory*. ASTM International, 2002.

19. ASTM Standard C 39, *Standard Test Method for Compressive Strength of Cylindrical Concrete Specimens*. ASTM International, 2003.

20. Japan Society of Civil Engineers, "Recommendations for Design and Construction of High Performance Fiber Reinforced Cement Composites with Multiple Fine Cracks (HPFRCC)," *Concr. Eng. Ser.*, vol. 82, p. Testing Method 6-10, 2008.

21. ASTM Standard C 1609, *Standard Test Method for Flexural Performance of Fiber-Reinforced Concrete (Using Beam With Third-Point Loading)*. 2005.

22. E. H. Yang, Y. Yang, and V. C. Li, "Use of high volumes of fly ash to improve ECC mechanical properties and material greenness," *ACI Mater. J.*, vol. 104, no. 6, pp. 620–628, 2007.

23. M. Maalej and V. C. Li, "FLEXURAL/TENSILE-STRENGTH RATIO IN ENGINEERED CEMENTITIOUS COMPOSITES," *J. Mater. Civ. Eng.*, vol. 6, no. 4, pp. 513–528, 1995.

24. Z. Zhang, S. Qian, H. Liu, and V. C. Li, "Ductile concrete material with self-healing capacity for jointless concrete pavement use," *Transp. Res. Rec. J. Transp. Res. Board*, no. 734, pp. 1–12, 2017.

25. L. Kan, H. Shi, A. R. Sakulich, and V. C. Li, "Self-Healing Characterization of Engineered Cementitious Composites Materials," *ACI Mater. J.*, vol. 107, no. 6, 2010.

26. S. Qian and V. C. Li, "Durable Pavement With Ecc," *1st Int. Conf. Microstruct. Relat. Durab. Cem. Compos.*, no. October, pp. 535–543, 2008.

APPENDIX A. TENSILE PROPERTIES STATISTICAL ANALYSIS

A1. Long-RECS15 Regular ECC (Tensile Strength and Strain Capacity)

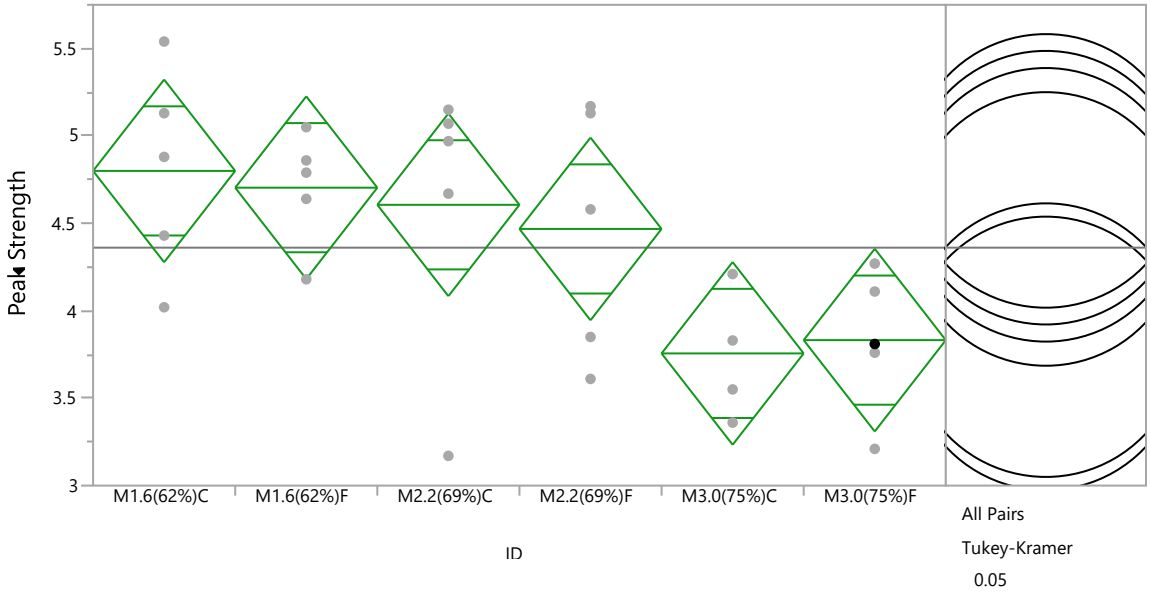

Figure 29. Long-RECS15 Regular ECC One-way Analysis (Tensile Strength).

Table 8. Long-RECS15 Regular ECC One-way ANOVA Results (Tensile Strength)

Source	DF	Sum of Squares	Mean Square	F Ratio	Prob > F
ID	5	5.138550	1.02771	3.2083	0.0234*
Error	24	7.687920	0.32033		
C. Total	29	12.826470			

Table 9. Long-RECS15 Regular ECC Tukey-Kramer HSD Connecting Letters Report (Tensile Strength)

Level		Mean
M1.6(62%)C	A	4.8000000
M1.6(62%)F	A	4.7040000
M2.2(69%)C	A	4.6060000
M2.2(69%)F	A	4.4680000
M3.0(75%)F	A	3.8320000
M3.0(75%)C	A	3.7560000

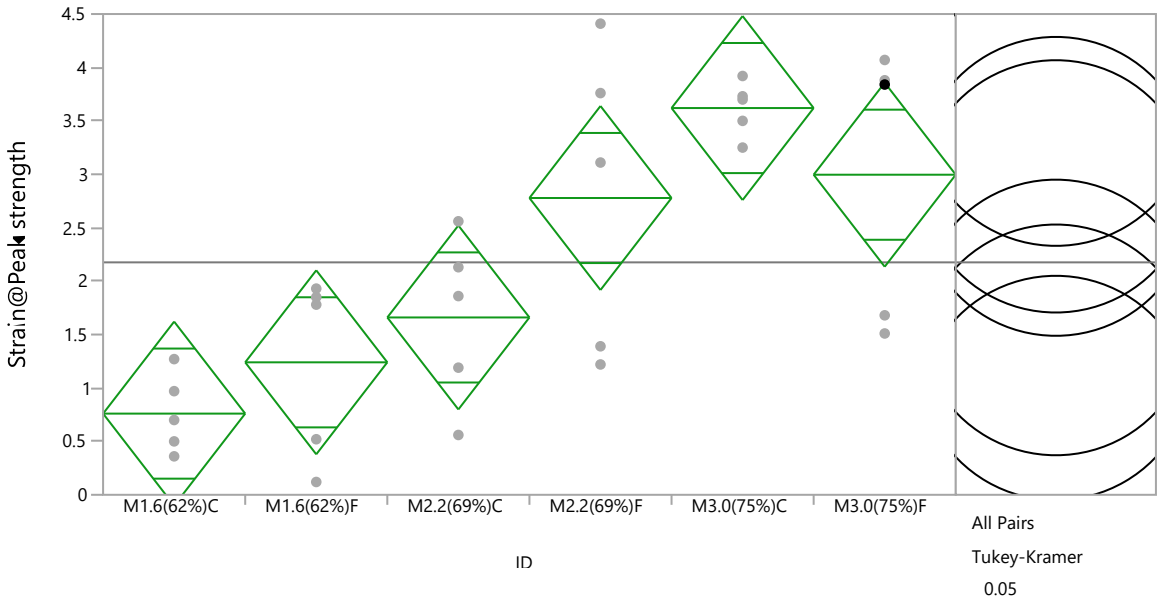

Figure 30. Long-RECS15 Regular ECC One-way Analysis (Strain Capacity).

Table 10. Long-RECS15 Regular ECC One-way ANOVA Results (Strain Capacity)

Source	DF	Sum of Squares	Mean Square	F Ratio	Prob > F
ID	5	31.336737	6.26735	7.2008	0.0003*
Error	24	20.888800	0.87037		
C. Total	29	52.225537			

Table 11. Long-RECS15 Regular ECC Tukey-Kramer HSD Connecting Letters Report (Strain Capacity)

Level				Mean
M3.0(75%)C	A			3.6200000
M3.0(75%)F	A	B		2.9960000
M2.2(69%)F	A	B		2.7780000
M2.2(69%)C		B	C	1.6600000
M1.6(62%)F		B	C	1.2400000
M1.6(62%)C			C	0.7600000

A2. Long-RECS15 Crumb Rubber ECC (Tensile Strength and Strain Capacity)

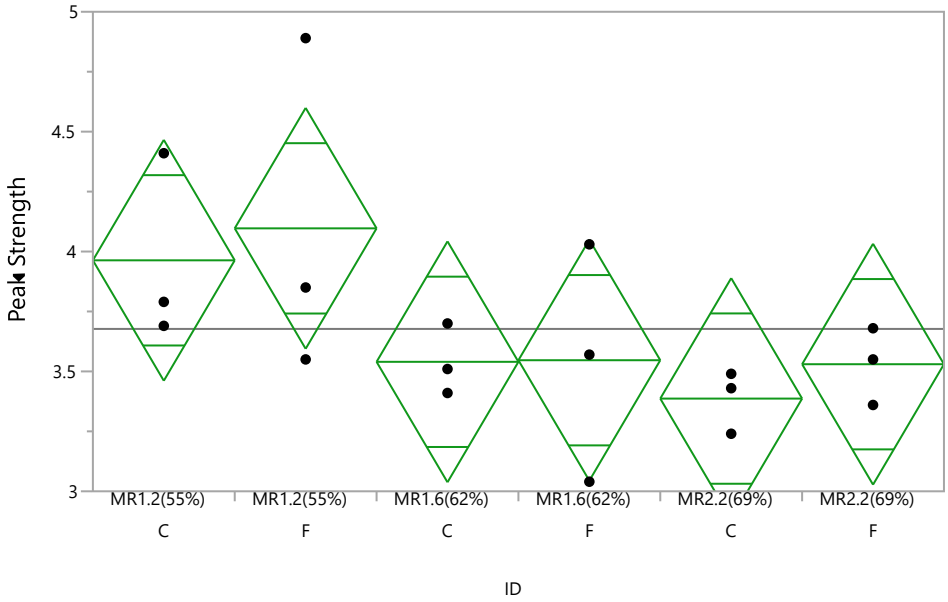

Figure 31. Long-RECS15 Crumb Rubber ECC One-way Analysis (Tensile Strength).

Table 12. Long-RECS15 Crumb Rubber ECC One-way ANOVA Results (Tensile Strength)

Source	DF	Sum of Squares	Mean Square	F Ratio	Prob > F
ID	5	1.1992944	0.239859	1.5042	0.2599
Error	12	1.9134667	0.159456		
C. Total	17	3.1127611			

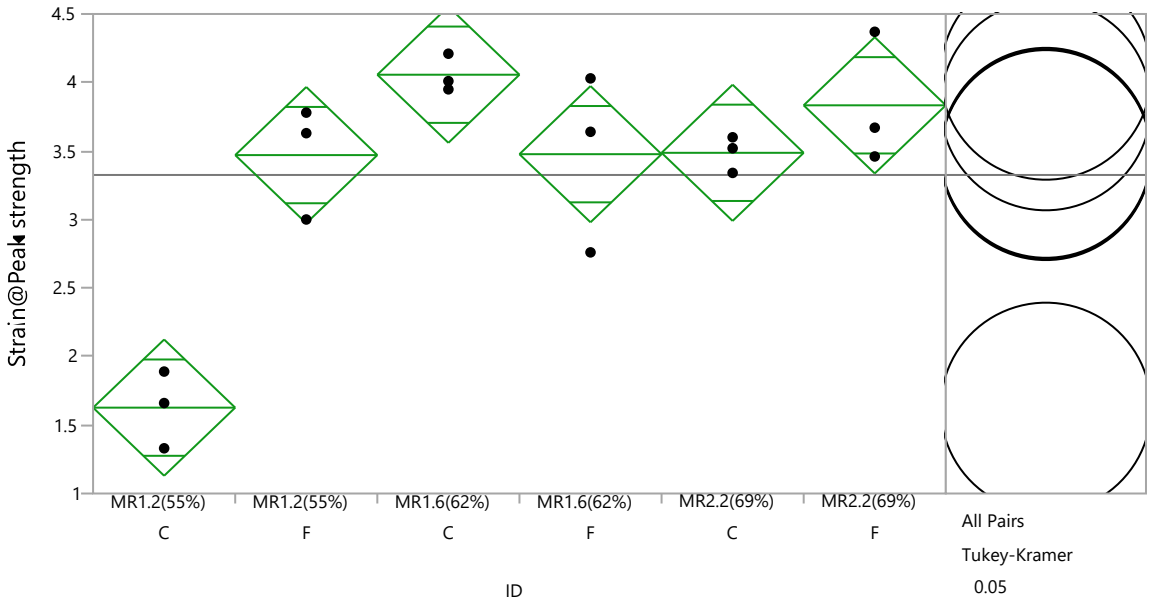

Figure 32. Long-RECS15 Crumb Rubber ECC One-way Analysis (Strain Capacity).

Table 13. Long-RECS15 Crumb Rubber ECC One-way ANOVA Results (Strain Capacity)

Source	DF	Sum of Squares	Mean Square	F Ratio	Prob > F
ID	5	11.244717	2.24894	14.3999	0.0001*
Error	12	1.874133	0.15618		
C. Total	17	13.118850			

Table 14. Long-RECS15 Crumb Rubber ECC Tukey-Kramer HSD Connecting Letters Report (Strain Capacity)

Level		Mean
MR1.6(62%)C	A	4.0566667
MR2.2(69%)F	A	3.8333333
MR2.2(69%)C	A	3.4866667
MR1.6(62%)F	A	3.4766667
MR1.2(55%)F	A	3.4700000
MR1.2(55%)C	B	1.6266667

A3. Short-RECS15 Regular ECC (Tensile Strength and Strain Capacity)

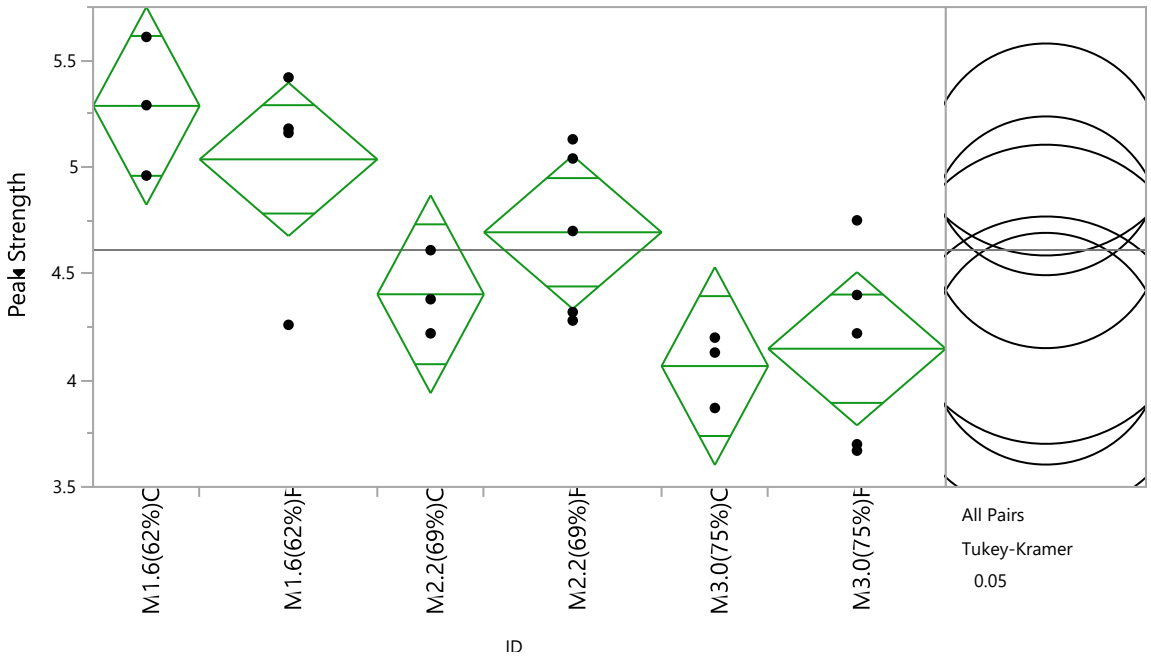

Figure 33. Short-RECS15 Regular ECC One-way Analysis (Tensile Strength).

Table 15. Short-RECS15 Regular ECC One-way ANOVA Results (Tensile Strength)

Source	DF	Sum of Squares	Mean Square	F Ratio	Prob > F
ID	5	4.3972633	0.879453	6.0165	0.0019*
Error	18	2.6311200	0.146173		
C. Total	23	7.0283833			

Table 16. Short-RECS15 Regular ECC Tukey-Kramer HSD Connecting Letters Report (Tensile Strength)

Level			Mean
M1.6(62%)C	A		5.2866667
M1.6(62%)F	A		5.0360000
M2.2(69%)F	A	B	4.6940000
M2.2(69%)C	A	B	4.4033333
M3.0(75%)F		B	4.1480000
M3.0(75%)C		B	4.0666667

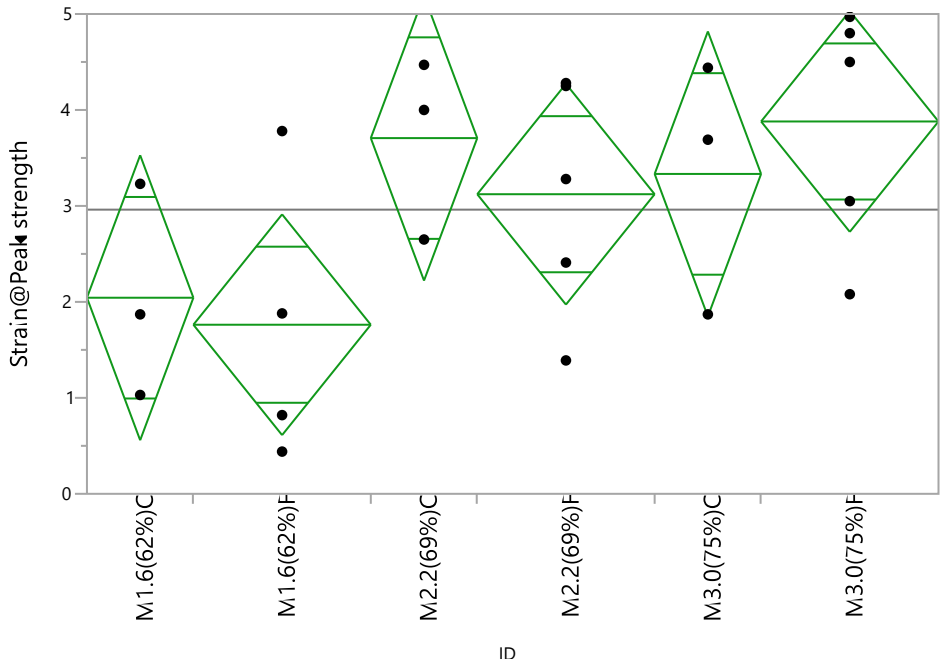

Figure 34. Short-RECS15 Regular ECC One-way Analysis (Strain Capacity).

Table 17. Short-RECS15 Regular ECC One-way ANOVA Results (Strain Capacity)

Source	DF	Sum of Squares	Mean Square	F Ratio	Prob > F
ID	5	16.150703	3.23014	2.1555	0.1051
Error	18	26.974160	1.49856		
C. Total	23	43.124863			

A4. Short-RECS15 Crumb Rubber ECC (Tensile Strength and Strain Capacity)

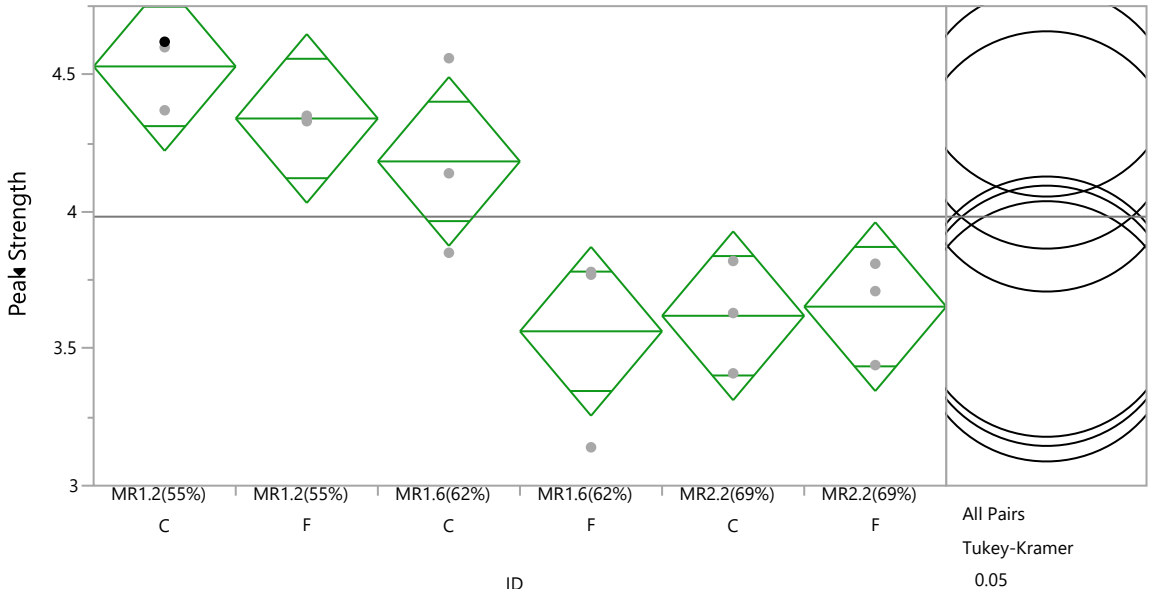

Figure 35. Short-RECS15 Crumb Rubber ECC One-way Analysis (Tensile Strength).

Table 18. Short-RECS15 Crumb Rubber ECC One-way ANOVA Results (Tensile Strength)

Source	DF	Sum of Squares	Mean Square	F Ratio	Prob > F
ID	5	2.6500500	0.530010	8.8335	0.0010*
Error	12	0.7200000	0.060000		
C. Total	17	3.3700500			

Table 19. Short-RECS15 Crumb Rubber ECC Tukey-Kramer HSD Connecting Letters Report (Tensile Strength)

Level			Mean
MR1.2(55%)C	A		4.5300000
MR1.2(55%)F	A		4.3400000
MR1.6(62%)C	A	B	4.1833333
MR2.2(69%)F		B	3.6533333
MR2.2(69%)C		B	3.6200000
MR1.6(62%)F		B	3.5633333

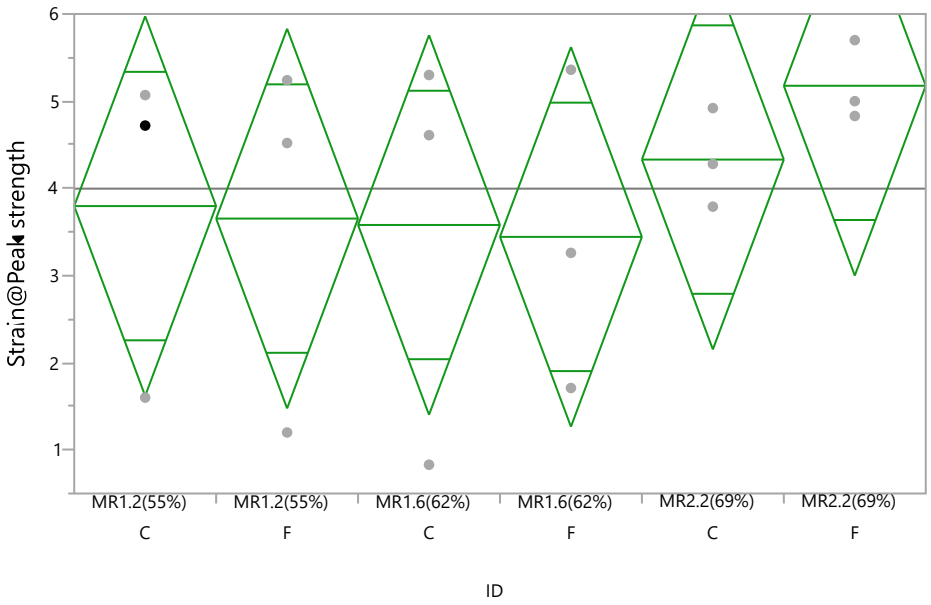

Figure 36. Short-RECS15 Crumb Rubber ECC One-way Analysis (Strain Capacity).

Table 20. Short-RECS15 Crumb Rubber ECC One-way ANOVA Results (Strain Capacity)

Source	DF	Sum of Squares	Mean Square	F Ratio	Prob > F
ID	5	6.423533	1.28471	0.4289	0.8201
Error	12	35.947667	2.99564		

APPENDIX B. FLEXURAL PROPERTIES STATISTICAL ANALYSIS

B1. Long-RECS15 Regular ECC (MOR and Deflection Capacity)

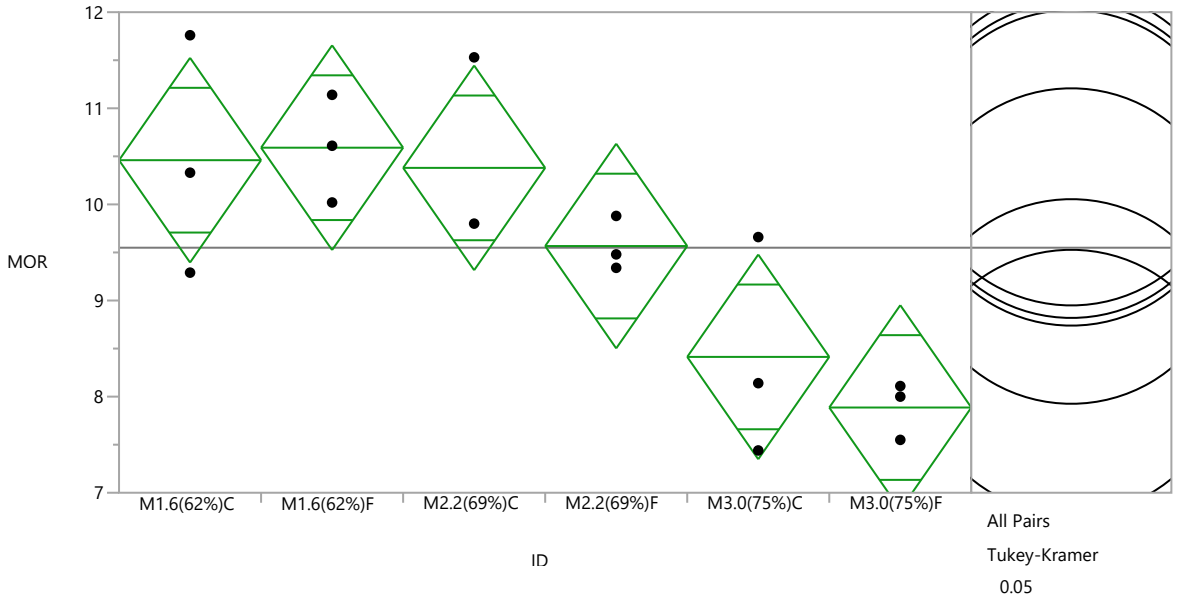

Figure 37. Long-RECS15 Regular ECC One-way Analysis (MOR).

Table 21. Long-RECS15 Regular ECC One-way ANOVA Results (MOR)

Source	DF	Sum of Squares	Mean Square	F Ratio	Prob > F
ID	5	19.972694	3.99454	5.5758	0.0070*
Error	12	8.596800	0.71640		
C. Total	17	28.569494			

Table 22. Long-RECS15 Regular ECC Tukey-Kramer HSD Connecting Letters Report (MOR)

Level			Mean
M1.6(62%)F	A		10.590000
M1.6(62%)C	A		10.460000
M2.2(69%)C	A		10.380000
M2.2(69%)F	A	B	9.566667
M3.0(75%)C	A	B	8.413333
M3.0(75%)F		B	7.886667

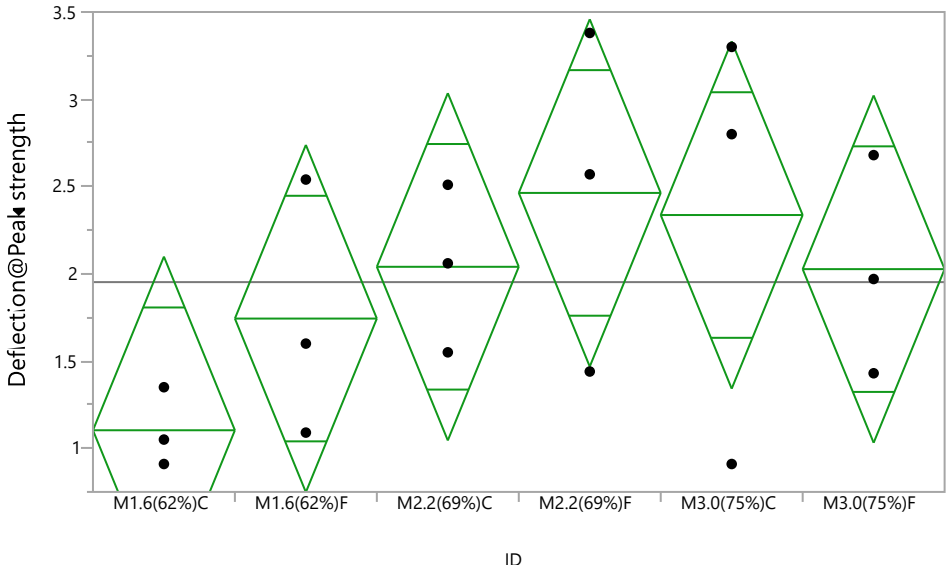

Figure 38. Long-RECS15 Regular ECC One-way Analysis (Deflection Capacity).

Table 23. Long-RECS15 Regular ECC One-way ANOVA Results (Deflection Capacity)

Source	DF	Sum of Squares	Mean Square	F Ratio	Prob > F
ID	5	3.559578	0.711916	1.1379	0.3926
Error	12	7.507533	0.625628		
C. Total	17	11.067111			

B2. Long-RECS15 Crumb Rubber ECC (MOR and Deflection Capacity)

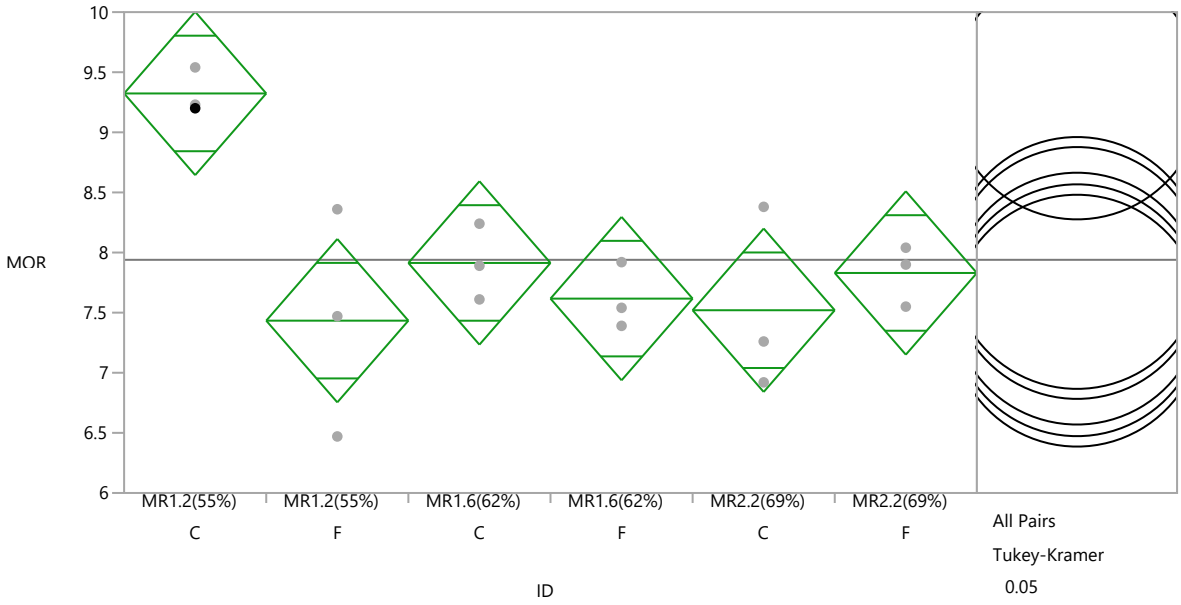

Figure 39. Long-RECS15 Crumb Rubber ECC One-way Analysis (MOR).

Table 24. Long-RECS15 Crumb Rubber ECC One-way ANOVA Results (MOR)

Source	DF	Sum of Squares	Mean Square	F Ratio	Prob > F
ID	5	7.392228	1.47845	5.0660	0.0100*
Error	12	3.502067	0.29184		
C. Total	17	10.894294			

Table 25. Long-RECS15 Crumb Rubber ECC Tukey-Kramer HSD Connecting Letters Report (MOR)

Level			Mean
MR1.2(55%)C	A		9.3233333
MR1.6(62%)C	A	B	7.9133333
MR2.2(69%)F		B	7.8300000
MR1.6(62%)F		B	7.6166667
MR2.2(69%)C		B	7.5200000
MR1.2(55%)F		B	7.4333333

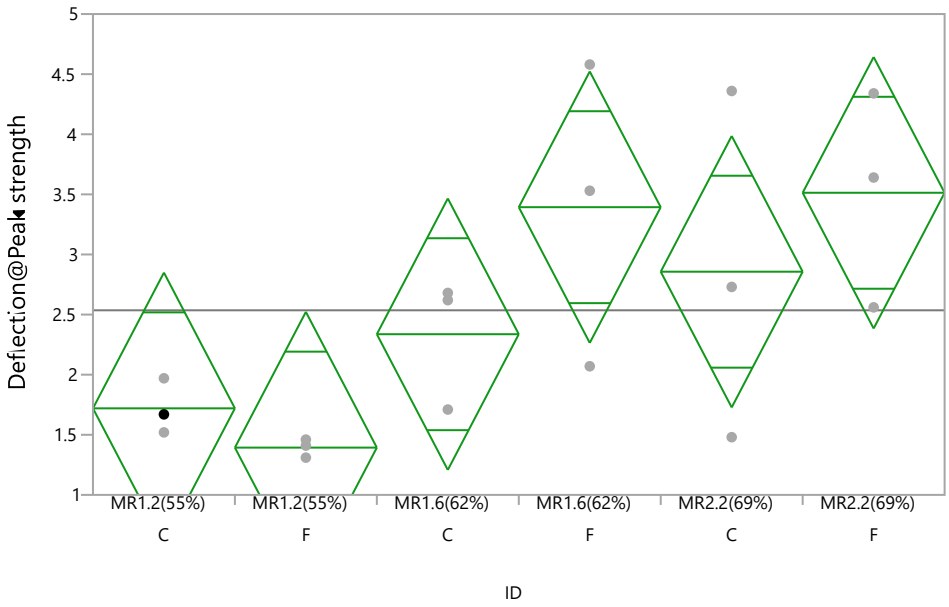

Figure 40. Long-RECS15 Crumb Rubber ECC One-way Analysis (Deflection Capacity).

Table 26. Long-RECS15 Crumb Rubber ECC One-way ANOVA Results (Deflection Capacity)

Source	DF	Sum of Squares	Mean Square	F Ratio	Prob > F
ID	5	11.412911	2.28258	2.8340	0.0647
Error	12	9.665133	0.80543		
C. Total	17	21.078044			

B3. Short-RECS15 Regular ECC (MOR and Deflection Capacity)

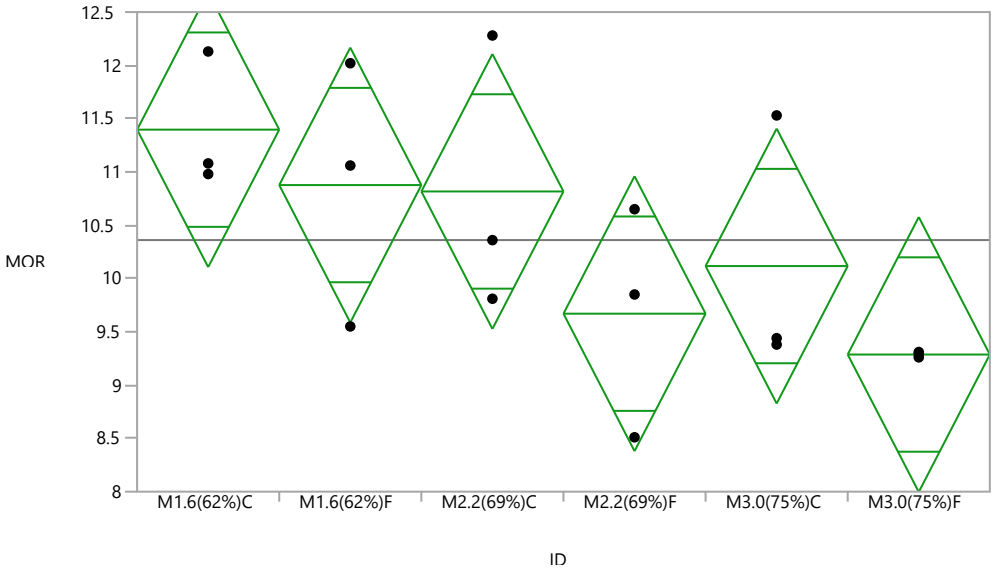

Figure 41. Short-RECS15 Regular ECC One-way Analysis (MOR).

Table 27. Short-RECS15 Regular ECC One-way ANOVA Results (MOR)

Source	DF	Sum of Squares	Mean Square	F Ratio	Prob > F
ID	5	9.712561	1.94251	1.8480	0.1778
Error	12	12.613533	1.05113		
C. Total	17	22.326094			

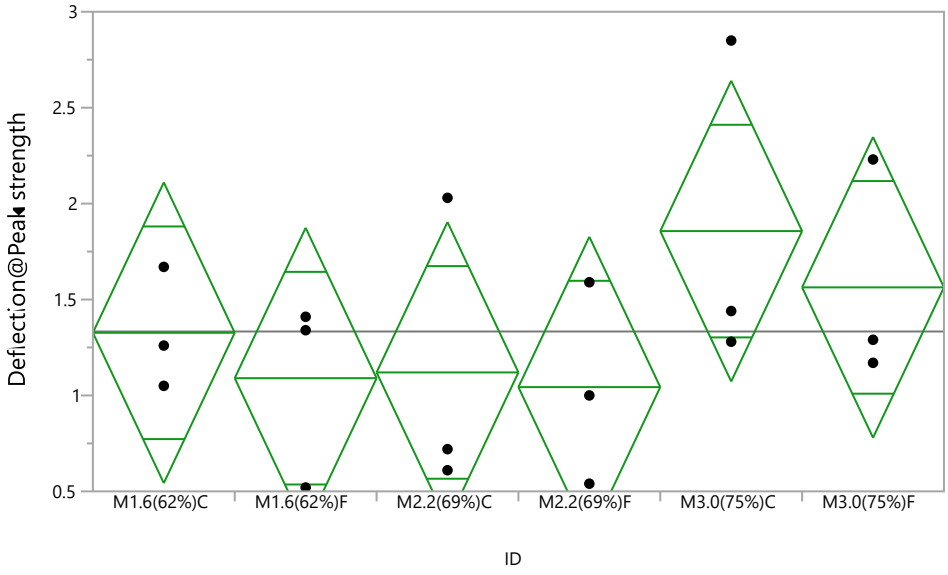

Figure 42. Short-RECS15 Regular ECC One-way Analysis (Deflection Capacity).

Table 28. Short-RECS15 Regular ECC One-way ANOVA Results (Deflection Capacity)

Source	DF	Sum of Squares	Mean Square	F Ratio	Prob > F
ID	5	1.5469333	0.309387	0.7971	0.5723
Error	12	4.6576667	0.388139		
C. Total	17	6.2046000			

B4. Short-RECS15 Crumb Rubber ECC (MOR and Deflection Capacity)

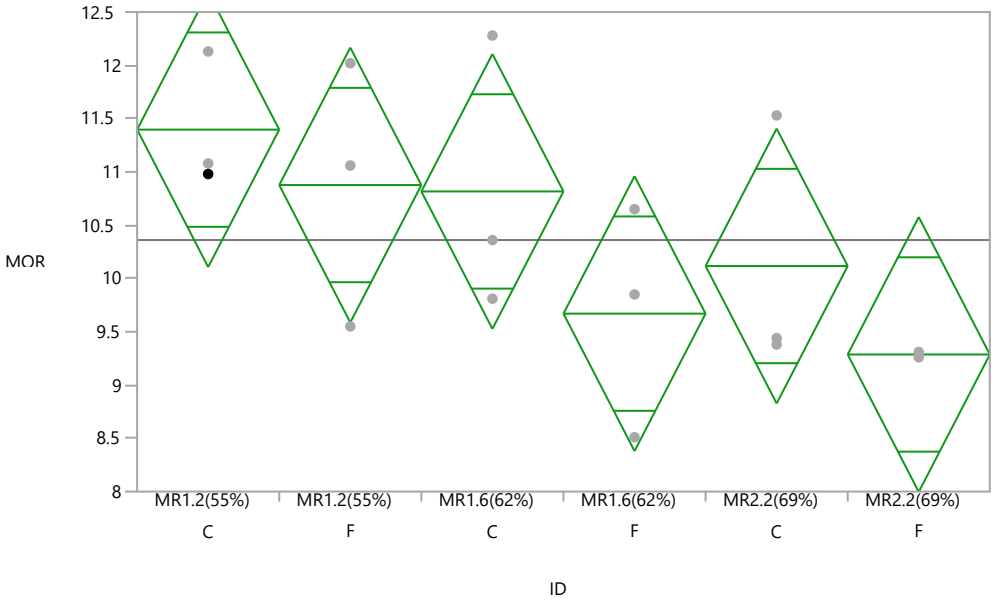

Figure 43. Short-RECS15 Crumb Rubber ECC One-way Analysis (MOR).

Table 29. Short-RECS15 Crumb Rubber ECC One-way ANOVA Results (MOR)

Source	DF	Sum of Squares	Mean Square	F Ratio	Prob > F
ID	5	9.712561	1.94251	1.8480	0.1778
Error	12	12.613533	1.05113		
C. Total	17	22.326094			

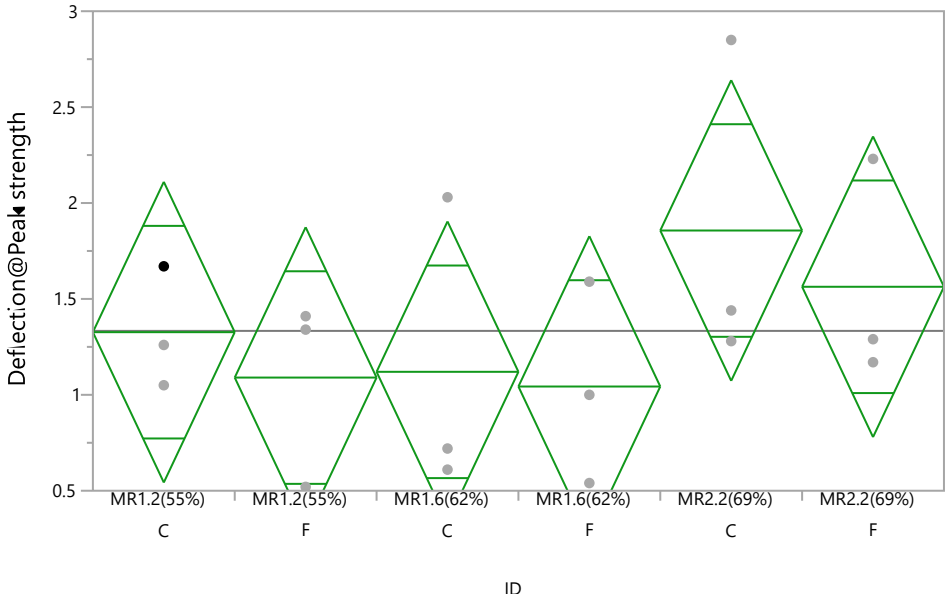

Figure 44. Short-RECS15 Crumb Rubber ECC One-way Analysis (Deflection Capacity).

Table 30. Short-RECS15 Crumb Rubber ECC One-way ANOVA Results (Deflection Capacity)

Source	DF	Sum of Squares	Mean Square	F Ratio	Prob > F
ID	5	1.5469333	0.309387	0.7971	0.5723
Error	12	4.6576667	0.388139		
C. Total	17	6.2046000			